The Journal of Experimental Biology 215, 3175-3190

doi:10.1242/jeb.072538

RESEARCH ARTICLE

Locomotion and behavior of Humboldt squid, *Dosidicus gigas*, in relation to natural hypoxia in the Gulf of California, Mexico

William F. Gilly[1,*], Louis D. Zeidberg[1,†], J. Ashley T. Booth[1,†], Julia S. Stewart[1], Greg Marshall[2], Kyler Abernathy[2] and Lauren E. Bell[1,§]

[1]Hopkins Marine Station of Stanford University, 120 Oceanview Boulevard, Pacific Grove, CA 93950, USA and
[2]National Geographic Society, Remote Imaging, Washington, DC 20036, USA

*Author for correspondence (lignje@stanford.edu)
†Current address: Department of Fish and Game, Marine Region, 20 Lower Ragsdale Drive, Suite 100, Monterey, CA 93940, USA
‡Current address: Department of Atmospheric and Oceanic Sciences, University of California, Los Angeles, CA 90095, USA
§Current address: P.O. Box 894, Homer, AK 99603, USA

SUMMARY

We studied the locomotion and behavior of *Dosidicus gigas* using pop-up archival transmitting (PAT) tags to record environmental parameters (depth, temperature and light) and an animal-borne video package (AVP) to log these parameters plus acceleration along three axes and record forward-directed video under natural lighting. A basic cycle of locomotor behavior in *D. gigas* involves an active climb of a few meters followed by a passive (with respect to jetting) downward glide carried out in a fins-first direction. Temporal summation of such climb-and-glide events underlies a rich assortment of vertical movements that can reach vertical velocities of 3 m s^{-1}. In contrast to such rapid movements, *D. gigas* spends more than 80% of total time gliding at a vertical velocity of essentially zero (53% at 0±0.05 m s^{-1}) or sinking very slowly (28% at –0.05 to –0.15 m s^{-1}). The vertical distribution of squid was compared with physical features of the local water column (temperature, oxygen and light). Oxygen concentrations of ≤20 μmol kg^{-1}, characteristic of the midwater oxygen minimum zone (OMZ), can influence the daytime depth of squid, but this depends on location and season, and squid can 'decouple' from this environmental feature. Light is also an important factor in determining daytime depth, and temperature can limit nighttime depth. Vertical velocities were compared over specific depth ranges characterized by large differences in dissolved oxygen. Velocities were generally reduced under OMZ conditions, with faster jetting being most strongly affected. These data are discussed in terms of increased efficiency of climb-and-glide swimming and the potential for foraging at hypoxic depths.

Key words: animal-borne video, foraging, jet propulsion, jumbo squid, movement, oxygen minimum zone, tagging.

Received 14 March 2012; Accepted 23 May 2012

INTRODUCTION

The Humboldt squid, *Dosidicus gigas*, is a large muscular squid with a rapid growth rate, a short life span and extremely high fecundity (Nigmatullin et al., 2001; Markaida et al., 2004; Argüelles et al., 2001). It is associated with highly productive, upwelling-driven ecosystems in the California and Peru Current Systems of the eastern Pacific Ocean (Roper et al., 1984). Throughout its large range (Canada to Chile) *D. gigas* plays an important ecological role as both predator and prey. In the Gulf of California, prey consists primarily of mesopelagic micronekton, including myctophid fishes, squids, pteropods and crustaceans (Markaida and Sosa-Nishizaki, 2003; Markaida et al., 2008), but this menu expands to include a variety of neritic and pelagic fishes in continental shelf and slope environments along the Pacific coast in the northern hemisphere (Field et al., 2007; Bazzino et al., 2010). In turn, *D. gigas* is a major prey item for sperm whales and other marine mammals, large teleost fishes and sharks, and is thus an important transitional organism in trophic webs, transferring energy from micronekton to the largest apex predators.

An important feature associated with most of the eastern Pacific Ocean is a well-defined oxygen minimum zone (OMZ), a midwater region where the concentration of dissolved oxygen is naturally lower than 20 μmol kg^{-1} (~0.5 ml l^{-1} or 0.7 mg l^{-1}) (Levin, 2003; Paulmier and Ruiz-Pino, 2009). This value is close to the concentration where microbial respiration switches from O_2 to NO_3^{-2} [~10 μmol kg^{-1} (Hofmann et al., 2011)] and is considered severely hypoxic for many nektonic organisms, including fishes, squids and crustaceans. The depth of the OMZ in the eastern Pacific varies with latitude (Helly and Levin, 2004) but typically extends from ~250 m to 1200 m in the southern half of the Gulf of California (Alvarez-Borrego and Lara-Lara, 1991). Control of oxygen concentration in the OMZ involves both physical and biological factors, including delivery of source water and microbial-based decomposition of sinking organic material in a deep, stable water column (Azam, 1998; Fiedler and Talley, 2006; Pennington et al., 2006; Karstensen et al., 2008; Paulmier and Ruiz-Pino, 2009). A variety of mesopelagic organisms, including myctophid fishes and krill, which constitute the main prey items of *D. gigas*, have adapted to conditions in the upper OMZ (Childress and Seibel, 1998; Drazen and Seibel, 2007), where they can avoid aerobic, visual predators during the day. This community of organisms comprises a major acoustic deep scattering layer (DSL) and generally undertakes a diel migration to near-surface waters to feed on plankton at night (Forward, 1988; Ringelberg, 1995; Benoit-Bird et al., 2009).

Table 1. Dates and locations of tag deployments and endpoints

Month/Year (Tag ID)	Sampling rate (Hz)	ML (cm)	Deployment Date (mm/dd/yy)	Deployment Latitude (°N)	Deployment Longitude (°W)	Endpoint Drifting (days)	Endpoint Date (mm/dd/yy)	Endpoint Latitude (°N)	Endpoint Longitude (°W)	Max. depth (m)	Max. distance (km)
10/04 (52869)	0.2	83	10/25/04	27.34	112.22	8	11/02/04	27.43	111.01	428	–
07/06A (61955)	1.0	74	07/11/06	27.33	112.21	1.5	07/12/06	27.43	111.43	336	75
07/06B (64006)	1.0	76	07/18/06	28.42	112.49	0	08/08/06	29.00	112.57	632	65
07/06C (60970)	1.0	79	07/17/06	28.42	112.46	–	–	–	–	590	–
03/07A (62007)	1.0	70	03/13/07	27.95	111.22	6	03/19/07	27.08	111.15	457	–
03/07B (62009)	1.0	75	03/13/07	27.95	111.22	0	03/29/07	26.59	109.87	1402	202
05/08 (64006)	0.5	~75	05/04/08	27.34	112.22	3	05/16/08	27.12	111.36	375	–
11/08A (64004)	0.5	77	11/16/08	27.53	112.32	1.1	11/30/08	27.64	111.27	1330	104
11/08B (83048)	1.0	79	11/16/08	27.53	112.32	0.8	11/28/08	28.62	112.115	445	123

Tags are named for month and year, i.e. Tag 10/04 was deployed in October 2004 (tag identifying numbers are in parentheses; tag 64004 was refurbished after recovery and redeployed). Endpoint is the location of the first signal sent to the Argos satellite. In most cases the tag detached prematurely and drifted at the surface until reporting to Argos after the number of indicated days spent drifting. Distances (straight line between deployment site and endpoint) were not computed if the tag drifted for more than 1.5 days before reporting to the satellite. Tag 07/06C never reported to Argos. Tag 07/06A released prematurely after only 36 h; data from this tag were not included in any further analysis.

Dosidicus gigas also migrates vertically in the water column, in a generally parallel fashion to that of the DSL, spending nighttime at shallow depths and daytime near the upper OMZ in the Gulf of California (Gilly et al., 2006) as well as in the Pacific Ocean off Baja California (Bazzino et al., 2010). Thus, *D. gigas* is potentially exposed to prey on a constant basis and may therefore be able to forage during both the day and the night. Although *D. gigas* can greatly reduce its resting metabolic rate in response to a cold, hypoxic challenge (Gilly et al., 2006; Rosa and Seibel, 2008; Rosa and Seibel, 2010), a previous tagging study did not detect any reduction in vertical velocities during daytime hours that were spent at very low oxygen (Bazzino et al., 2010). Effects of hypoxia on the metabolic rate of *D. gigas* during active swimming are not known, but presumably highly aerobic activity such as high-velocity jetting would be significantly impaired in the OMZ.

In this paper we address this puzzle by deploying electronic tags of improved resolution and an animal-borne video package (AVP) in different locations and seasons in the Guaymas Basin of the Gulf of California that are characterized by large differences in the depth of the upper OMZ. This allows a thorough analysis of the vertical distribution of *D. gigas* in relation to this environmental feature and provides new insight into the patterns and speed of vertical movements. Nearly all locomotion by *D. gigas* appears to involve fins-first active ascents and passive descents in a pattern of classic 'climb-and-glide' swimming (Weihs, 1973). Temporal summation of small climb-and-glide events underlies complex and rapid swimming behaviors in all parts of the water column, including the OMZ, but vertical velocities across a wide range are clearly reduced in the upper OMZ. We also find that when the upper OMZ is deeper than ~300 m, Humboldt squid decouple from this feature and spend daytime at shallower depths, which are not as severely hypoxic. In these cases, light and presumably the presence of the DSL probably act to determine the daytime habitat of this species.

MATERIALS AND METHODS

Animals

Humboldt squid [*Dosidicus gigas* (D'Orbigny 1835)] were captured from research vessels in the Guaymas Basin (including its northern extension, known as the San Pedro Martir Basin) of the Gulf of California, Mexico, between 2004 and 2008 using conventional rod-and-reel or hand-line methods with weighted, luminescent jigs. Squid were brought on deck or held next to the vessel and assessed for suitable size for tagging [>70 cm dorsal mantle length (DML)] or AVP deployment (>80 cm DML) before proceeding as described below. Care was taken to ensure vitality of a tagged squid by holding it gently beneath the surface until it showed a burst of powerful jetting. Squid for tagging were caught after dusk; squid for AVP deployments were captured in mid-afternoon.

Archival tags

Pop-up archival transmitting (PAT) tags (Wildlife Computers, Redmond, WA, USA) were attached to the medial-ventral surface of a fin as described elsewhere (Gilly et al., 2006). Animals were tagged on deck with constant irrigation of the gills with ambient seawater. MK10 tags with 1 Hz sampling were used in most cases, and these devices measure depth from 0 to 2000 m with a resolution of 0.5 m and temperature from 0 to +40°C with a resolution of 0.05°C. Two PAT4 tags were also used (10/04 and 07/06B in Table 1). Depth resolution of these tags ranges from 0.5 m (0–100 m range) to 8 m (for depths >400 m). Only data from MK10 tags with 1 Hz sampling were used for analysis of vertical velocity at different depths.

Eleven of 13 tags deployed in the course of this study reported summary data to the Argos satellite system. Nine tags were physically recovered, and the complete archival data sets were analyzed (Fig. 1, Table 1). These tags are referred to by their month and year of deployment (mm/yy). Four tags were deployed in the vicinity of Santa Rosalia, Baja California Sur (10/04, 05/08, 11/08A,B), two off Guaymas, Sonora (03/07A,B), and three near Isla San Pedro Martir (07/06A,B,C). To compare swimming behavior and vertical distribution of individual squid with independently assessed hydrographic properties (oxygen and temperature), we analyzed vertical distribution and velocities for the first 3 days, which was assumed to be a reasonable time for the squid to remain in an area with similar conditions to those in the area of the tag deployment where the hydrographic surveys were made.

Tags 10/04 and 07/06C were recovered opportunistically and returned for a reward. All other tags were recovered through active searches at sea using a radio direction-finding system based on a mast-mounted antenna (DDF6095) and display processor (DDF6001F, Doppler Systems, Carefree, AZ, USA) and receiver (PRO-97, Radio Shack, Fort Worth, TX, USA) that allowed localization of the 401.650 MHz transmissions by the floating tag to Argos satellites. Updated tag positions were accessed through the internet using a portable satellite phone. We relied on a hand-held Argos receiver (TSUR-400, Telonics, Mesa, AZ, USA) to

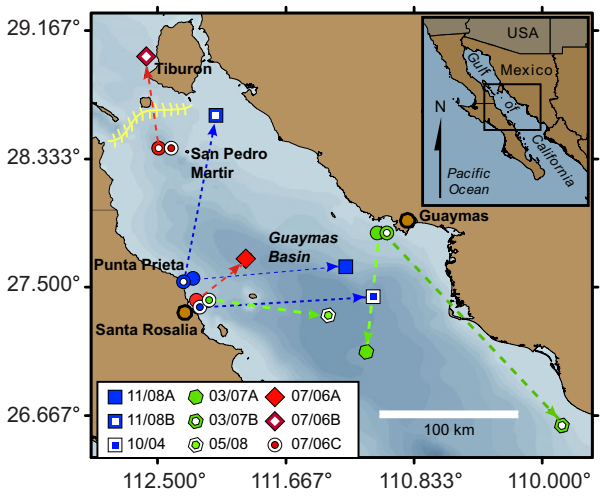

Fig. 1. Pop-up archival transmitting (PAT) tag deployment and endpoint positions. Tags were deployed on *Dosidicus gigas* near the fishing ports of Santa Rosalia, Baja California Sur, and Guaymas, Sonora. Circles indicate deployment locations, and symbols identified in the legend show endpoint locations as determined by the first location provided by Argos. Red symbols denote tags deployed in summer (July), blue denotes fall deployments (October and November), and green denotes spring deployments (March and May). Dotted arrows indicate straight-line distances between deployment and endpoints. Yellow herringbone pattern denotes a sill that extends to ~200 m depth. The deepest portion of the Guaymas Basin is ~2000 m (area of endpoint for tag 05/08). The lightest shading represents depths of <200 m (endpoint for 11/08B).

provide the final, close-range detection (generally several hundred meters) of the tag before commencing a dedicated visual search. Floats of the tags were painted International Orange to facilitate visual detection. Before each search, the radio direction-finding system was calibrated in place on the vessel using a SPOT5 tag (Wildlife Computers) to provide an Argos signal, typically from a distance of 100–200 m.

Tag data were analyzed with MATLAB (MathWorks, Natick, MA, USA), IGOR Pro (WaveMetrics, Eugene, OR, USA) and a custom graphical user interface (L. Giovangrandi, Electrical Engineering, Stanford University, CA, USA) that allows visualization and specific transformations of data. Vertical velocity was computed for those PAT tags with 1 Hz sampling as the simple, two-point time derivative of depth after smoothing the depth record with a Savitsky–Golay filter (order=6, frame size=33).

Animal-born video package

National Geographic's Crittercam (Marshall et al., 2007) was deployed on three squid in September 2009 at Punta Prieta north of Santa Rosalia (27.54°N, 112.3°W; see Fig. 1). This AVP (0.7 kg in air, 25.4×5.7 cm) is capable of storing digital black-and-white video (17 Hz) and logging sensor data at 1 Hz for temperature, depth, light and acceleration along three mutually orthogonal axes. The instrument package was fitted onto an animal being gently held at the surface behind the vessel's dive platform. A sleeve of stretchable nylon fabric (57.5 cm circumference), attached to a thin fiberglass sheet for docking the AVP, was slid over the mantle from the posterior (fins) end, and slack was taken up by cinching the sleeve with plastic cable ties in a way so as not to restrict normal mantle movements. The assembly was positioned so the docking sheet was located on the dorsal midline, and the sheet was then secured to the anterior edge of mantle on each side of the gladius by a cable tie looped through the muscle ~1 cm from the mantle edge and 4 cm from the midline. Finally, a syntactic foam cradle holding the Crittercam was attached to the docking plate by a programmable release mechanism. Software for programming the AVP and uploading data were provided by National Geographic's Remote Imaging Unit.

Two AVP deployments (nos 2 and 3) were made during daytime with no artificial lighting, and this allowed video observations under natural lighting conditions. Vertical movements were comparable to those recorded with PAT tags, indicating that the squid were not significantly impaired by the AVP. This is also suggested by a variety of social interactions between the squid carrying AVP 3 and a group of conspecifics that was encountered (see Results). Deployment of AVP 1 was carried out at night using red LEDs as a light source, but this squid was quickly attacked by a group of conspecifics. The use of artificial lighting was therefore abandoned, and data from AVP 1 are not considered in this paper.

Following its timed release and appearance at the surface, the AVP was located using a directional Yagi-type antenna to detect a VHF beacon. Video playback and editing was managed with the VLC media player (v1.1.2, VideoLan Project, Paris, France) and Adobe Premiere Pro CS4 (v4.2.1, Adobe Systems, San Jose, CA, USA). Image analysis was conducted using ImageJ (v1.42q, National Institutes of Health, Bethesda, MD, USA) and IGOR Pro software. Sensor data were analyzed with IGOR Pro and original programs in both MATLAB and R (v2.12.2, The R Foundation for Statistical Computing, Vienna, Austria).

Vertical velocity was computed as the time derivative of depth as described above. Pitch was defined as the angle between the squid's longitudinal axis (in the arms-to-fins direction) and a plane parallel to the sea surface, with positive angles being upward. When the squid is actively jetting in a fins-first direction, pitch is equivalent to the angle of inclination that describes the overall trajectory of the moving animal. This is not necessarily the case at all times (see Results).

Pitch was calculated from raw tri-axial acceleration data (A_x, A_y and A_z) as $\arctan[A_x/(A_z^2+A_y^2)^{-1/2}]$. Absolute pitch angles from this analysis must be regarded as approximate, because data from tri-axial accelerometers alone cannot distinguish between static movements (i.e. pitch, roll) and small accelerations in a particular direction that would be generated by active jetting. Pitch measurements were deemed valid if values for $(A_x^2+A_y^2+A_z^2)^{1/2}$ deviated from 1.0 by less than 10% (Marshall et al., 2007). Most deviations outside this range lasted only for a few seconds. Video data were also used to confirm orientation of the squid relative to the surface based on background light intensity.

Oceanographic measurements

Hydrographic measurements at the sites of tag deployment were made on the same day to a maximum depth of 600 m with an SBE19plus conductivity-temperature-depth (CTD) profiler equipped with an SBE43 oxygen sensor that was calibrated annually (Seabird Electronics, Bellevue, WA, USA). Additional profiles were obtained over the course of several days preceding and following tag deployment. In several cases profiles were also made at the time of tag recovery. These data were analyzed with IGOR Pro and were imported into Ocean Data View 4 (http://odv.awi.de) for further analysis and plotting.

Sea surface temperatures throughout the year were measured in the Santa Rosalia area by monthly CTD casts during 2007–2008 (except August and September) using the equipment described in the previous paragraph.

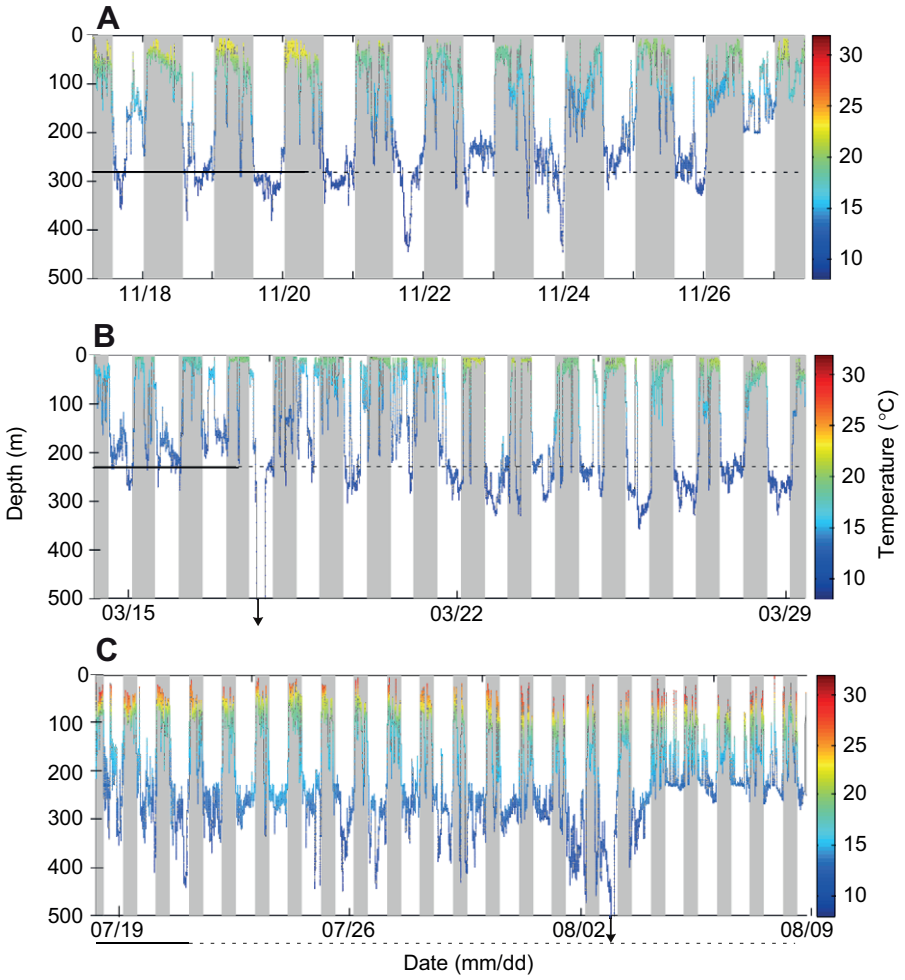

Fig. 2. Examples of complete time-series records of depth (and color-coded temperature data) for tags deployed on *Dosidicus gigas* in different seasons. In each panel, the depth of the oxygen minimum zone (OMZ) in the vicinity of the deployment site is indicated by the dashed horizontal line and the solid line during the first 3 days. (A) Autumn deployment (tag 11/08B) in the Santa Rosalia area. (B) Spring (tag 03/07B) deployment in the Guaymas area. The deep dive on the fourth day (arrow) reached a depth of 1400 m (see Table 1). (C) Summer deployment (tag 07/06B) near Isla San Pedro Martir. This squid moved from the Guaymas Basin across the sill indicated in Fig. 1 to an area west of Isla Tiburon where the tagged popped up. The deep dive on 3 August (arrow) reached a depth of 630 m (see Table 1).

RESULTS

Locomotion and behavior

General activity patterns

In agreement with a previous study in this general location (Gilly et al., 2006), all of the squid carrying PAT tags generally spent nighttime at shallower depths than in the daytime and showed reliable movements towards the surface at dusk and back to depth at dawn. These overall features are evident in typical time-series data (Fig. 2). Although the diel migration pattern is clear, there is much high-frequency vertical movement, both at depth during the day and close to the surface at night. Physical features of the midwater environment will be established in the second part of this paper and related to squid distribution and behavior at that time.

General mechanics of swimming: climb-and-glide

Swimming by loliginid squid, coastal inhabitants that are much smaller than *D. gigas*, involves an active and complex combination of jet propulsion and fin beating at most swimming speeds (Bartol et al., 2001a; Bartol et al., 2001b; Anderson and DeMont, 2005; Bartol et al., 2008). In general, lower speeds involve more fin undulation and beating, whereas the highest speeds do not involve the fins at all (Hoar et al., 1994). In all cases, a cycle of jet propulsion involves inhalation of water into the mantle cavity, sometimes assisted by contraction of radial muscle fibers, followed by exhalation through the siphon driven entirely by contraction of circular muscle. The siphon is muscular and can aim in any direction, so jet-propelled movement can be fins-first or arms-first, with similar maximum velocities in both directions (Packard, 1969). Positive acceleration due to jetting occurs only during exhalation. Gliding, often accompanied by fin beating, occurs during refilling, making movement inherently pulsatile. The larger the squid, the more useful gliding will be as a component of locomotion, and a tagged *D. gigas* is a large squid with a mass of 20 kg or more.

Although the extensive archival records from PAT tags provide the richest variety of vertical movements over a large depth range, the basic features of locomotion are more readily explained in conjunction with squid carrying the AVP. Fig. 3A represents the complete depth (black, upper) and velocity (blue, lower) records obtained with AVP 2. After descending to ~100 m immediately after its release (arrow), the squid remained near this depth for ~1 h before beginning a gradual ascent to ~50 m. Vertical velocity transients of up to 1.0 m s^{-1} peak amplitude are evident throughout this period. One such event (segment B) is expanded in Fig. 3B. A smooth climb of 3 m and associated velocity spike of 0.5 m s^{-1} peak amplitude occurs in the middle of a slow descent with a mean (±s.d.) velocity of –0.056±0.039 m s^{-1} (excluding 20 points associated with the velocity transient). Analysis of the squid's pitch (red traces and diagrams in Fig. 3B,C) indicates that the squid climbed in a fins-first direction at an inclination angle of 68 deg, tilted downward briefly (negative pitch angle) at the apex of the climb and then quickly assumed a pitch of near 0 deg during the subsequent slow descent.

Based on examination of many such records from both AVP and PAT depth sensors, we regard the event shown in Fig. 3B as representing the fundamental pattern of vertical movement – an

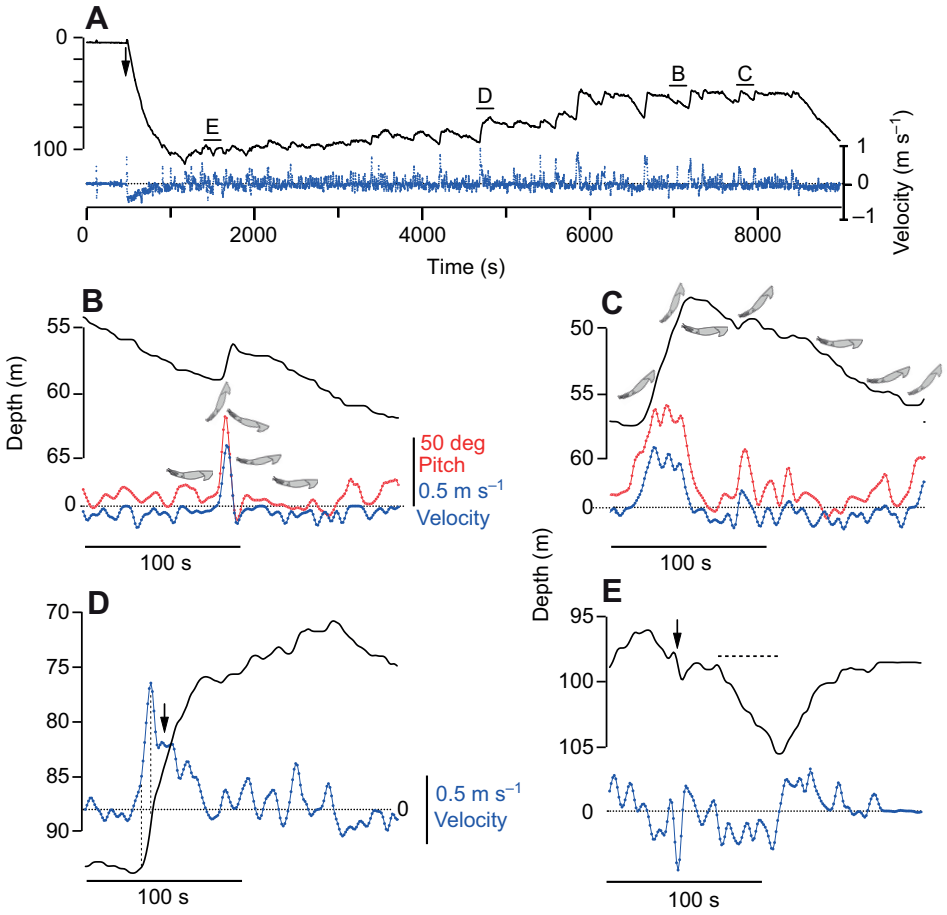

Fig. 3. Climb-and-glide swimming behavior in *Dosidicus gigas*. In all panels, depth is the black uppermost trace, and vertical velocity is the blue lowermost trace. (A) Complete depth and vertical velocity records for animal-borne video package (AVP) 2. Segments labeled B–E correspond to panels B–E where they are displayed at higher vertical and horizontal resolution. (B) A single elemental jetting event in which a brief velocity spurt is associated with a discrete upward movement at positive pitch (red, middle trace and diagrams) followed by prolonged sinking at very low velocity and nearly zero pitch. Vertical scale bars for pitch and velocity represent absolute values of magnitude; dotted line equals zero for both. (C) A larger smooth ascent is followed by a more complex pattern of gliding. See B for a vertical scale bar. (D) Records for depth and vertical velocity during a maintained climb of variable speed. Arrow indicates an example of a smooth climb with little or no visible deceleration phase between jets. (E) Depth and vertical velocity records corresponding to active descents (arrow and dashed line). See D for a velocity scale bar.

active fins-first ascent, characterized by a brief (~10 s duration) velocity transient of ≥0.3 m s^{-1} followed by much longer-lasting, slow descent at ~0.05 m s^{-1}. We assume that the slow sinking phase is essentially passive with respect to jetting for these slightly negatively buoyant animals. Fin beating probably occurs in combination with both jetting and gliding, but we cannot address its contribution to locomotion based on available data.

Although we discuss these events in terms of a single functional 'jet' during the ascent, it is likely that several cycles of contraction and partial relaxation are smoothly integrated to a degree that prohibits discrimination of the individual pulses. An alternative mechanism would be repetitive opening and closing of the siphon during a single cycle of mantle contraction, and this would likewise deliver pulses of thrust. These mechanisms could also be combined. Given that the inhalation rate under laboratory conditions at 7–10°C is ~0.33 Hz [unpublished data collected in conjunction with a previous study (Gilly et al., 2006)] and that siphon diameter is actively controlled in free-swimming animals (see Depth-maintenance behavior below), a combination of these mechanisms seems most likely. At present, we cannot specify the biomechanical details of the ascent phase of these individual 'jetting events'.

This pattern of active ascent and passive descent defines classic 'climb-and-glide' locomotion seen in many flying and swimming organisms (Weihs, 1973). Repetitive respiratory movements of seawater into and out of the mantle cavity must occur during passive sinking occurring over such long periods, but evidently these events are too weak (or the siphon is oriented horizontally) to generate detectable vertical velocity transients. Based on observations in large tanks (W.F.G., personal observation) and from remotely operated vehicles (ROVs) (L.D.Z., personal observation), fin posture and activity can control the rate of descent, but this factor has not been quantitatively studied. We have no direct information regarding horizontal velocities with either AVP or PAT tag sensors, but some estimates can be made, as described in the next section.

Discrete climb-and-glide motions of this sort are the 'elemental' events out of which more complex behaviors are built. An ascent and descent of 10 m are illustrated in Fig. 3C. It is clear from inspection that the climb is composed of at least three elemental-type jetting events, as evidenced by the discrete peaks in the associated velocity transient. Larger steady climbs can thus be generated through temporal summation of small elemental events in a way that results in a relatively smooth velocity transient that is maintained throughout the ascent. Refilling of the mantle presumably occurs during the brief deceleration phase between individual jets, but it is unlikely that one or even several jets of this modest amplitude would deplete much of the seawater in the mantle cavity.

Varying the timing between jetting events, as indicated by the peaks of velocity transients, can control the rate of ascent, as demonstrated in Fig. 3D. Faster motion is generated by decreasing the time between mantle contractions to the point that little or no deceleration phase is visible (arrow), and the subsequent increase in time between jetting events during the second half of the record results in a slower rate of climb with little or no gliding. All of the above features of elemental events and their temporal summation are also seen in conjunction with active descents (Fig. 3E). A rapid downward jetting event is evident (arrow), and the smaller negative velocity transients during the subsequent descent (dashed line) are

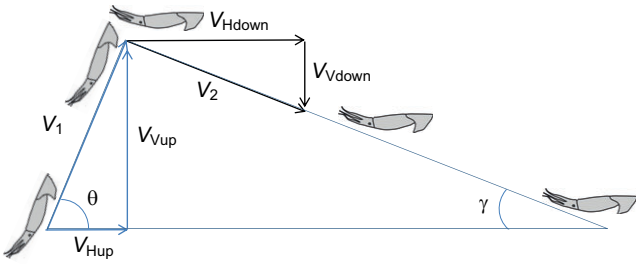

Fig. 4. Schematic climb-and-glide event and the components of velocity during the ascent (up) and descent (down) of *Dosidicus gigas*. Distances and times associated with these velocities are described in the text (see Horizontal movement during climb-and-glide swimming). Angles of the trajectory during the climb (θ) and glide (γ) are indicated.

associated with a mean descent rate of 0.16±0.07 m s^{-1}, a value threefold faster than that associated with passive sinking.

It appears from records such as these that *D. gigas* extensively utilizes temporal summation of active jetting events and passive glides to carry out virtually all of its vertical movements. Elemental jetting events, as defined by the overall time course of the associated velocity transient (~10 s), can also vary somewhat in peak velocity (0.3 to 1 m s^{-1}; see initial event between vertical dashed lines in Fig. 3D), and this represents another mechanism for controlling overall velocity. This ability simply requires adjustment of the velocity of mantle contraction over a fixed time corresponding to an elemental event (~10 s).

Horizontal movement during climb-and-glide swimming

An estimate of horizontal motion during a single climb-and-glide event can be derived from the changes in depth and pitch during individual events during the AVP deployments. A schematic event is illustrated in Fig. 4. Measurements of 27 such events from the AVP deployments with a vertical ascent of ≥1 m and similar descent showed a vertical (upward) movement (d_{Vup}) of 2.2±0.2 m (mean ± s.e.m.) traversed in 9.1±0.9 s (t_{up}), corresponding to a vertical velocity (V_{Vup}) of 0.27±0.02 m s^{-1}. Measured pitch angle for these climbs was 51.0±2.5 deg, and this value would equal the angle of inclination (θ). Pitch ranged from 30.5 to 77.8 deg, with higher angles more likely to be associated with longer ascents (data not shown). Descents occurred with the squid maintaining a posture of nearly zero pitch over a similar vertical distance (1.8±0.1 m) but much longer time (37.4±3.3 s) (t_{down}), defining an angle of glide (γ). Vertical velocity during the descent (V_{Vdown}) was –0.054±0.004 m s^{-1}, a value characteristic of passive sinking. In the following discussion, vertical ascent and descent distances are assumed to be equal for simplicity.

Based on the average values for V_{Vup} (0.27 m s^{-1}), pitch (51 deg) and upward movement (d_{Vup}=2.2 m), the horizontal velocity component of the ascent (V_{Hup}) is given by:

$$V_{Hup} = V_{Vup} / \tan\theta = 0.22\,\text{m s}^{-1}, \quad (1)$$

and the horizontal distance traveled during the ascent (d_{Hup}) would be:

$$d_{Hup} = V_{Hup} t_{up} = 2.0\,\text{m}. \quad (2)$$

Velocity in the direction of travel (V_1) is then:

$$V_1 = V_{Vup} / \sin\theta = 0.35\,\text{m s}^{-1}. \quad (3)$$

Horizontal movement during the descending glide can be estimated as the product of the horizontal velocity component of descent (V_{Hdown}) and the measured value of t_{down}. Pitch angle is not useful for the descent, because it is essentially zero. If we assume that the squid continues moving with a horizontal velocity that is a fraction (α) of V_1 after changing its pitch at the apex of the climb, then the horizontal distance traveled during the descent (d_{Hdown}) is:

$$d_{Hdown} = \alpha V_1 t_{down}. \quad (4)$$

For α=0.75 (i.e. 25% of forward velocity V_1 is lost in turning at the apex), d_{Hdown} following the 2.2 m vertical ascent would be 9.8 m, and the total horizontal distance traveled during the climb-and-glide event would be the sum of d_{Hup} and d_{Hdown}, in this case 11.8 m. The overall angle of glide (γ) would be:

$$\gamma = \arctan(d_{Vup} / d_{Hdown}) \approx 13\,\text{deg}. \quad (5)$$

This approach is admittedly simplistic, neglecting drag and other factors during the descent, including weak, horizontally directed respiratory jets and fin activity, but it provides a rough lower estimate of horizontal motion that can be considered in conjunction with data from tags. Overall horizontal velocity during the climb-and-glide event would be given by $(d_{Hup}+d_{Hdown})/(t_{up}+t_{down})$=11.8/46.5=0.25 m s^{-1} for α=0.75. For values of α ranging from 0.5 to 1.0, horizontal velocities would vary from 0.23 to 0.32 m s^{-1}, respectively. This range is consistent with that observed with more direct measurement methods (see Discussion).

Depth-maintenance behavior

Tagged squid (both AVP and PAT tags) often maintained their position in the water column for a considerable period of time over a narrow depth range. This behavior is evident throughout much of the depth records for both AVP deployments (Fig. 3A, Fig. 5A) and generally involves repetitive episodes of upward jetting and passive sinking, i.e. climb-and-glide. We operationally defined depth-maintenance behavior as maintaining vertical position within a range of ±15 m for at least 15 min. Typically, depth maintenance is carried out through simple climb-and-glide behavior (Fig. 5B) interspersed with other types of motions, such as the brief arms-first ascent at negative pitch (up arrow and diagram) and the quick downward jet toward the end of the record (down arrow).

Based on the above definition, squid carrying MK10 PAT tags spent 9.7±1.6% (mean ± s.e.m., *N*=7) of the total deployment time engaged in depth-maintenance behavior, with values ranging from 3.4% (tag 07/06B) to 18.5% (tag 03/07A). Bouts of depth maintenance occurred during both day and night, at all depths, and often occurred in clusters (data not shown). Durations of ascents were typically 10–40 s, and descents ranged from 20 to 150 s, with no consistent nature to the frequency distribution of durations. Vertical velocities during ascents and descents during depth maintenance were each exponentially distributed with means of ~0.5±0.1 and –0.15 m s^{-1}, respectively. Velocity distributions will be discussed in relation to oxygen concentrations at different depths in a following section (see Effects of OMZ conditions on vertical velocity).

One function for depth-maintenance behavior was demonstrated during the final 20 min of AVP 3 deployment (Fig. 5A,C) when the squid encountered a sizeable group of conspecifics at a depth of 50 m. During this period of extremely tight depth maintenance, there was little sign of canonical climb-and-glide swimming. Instead, the squid displayed a variety of rapid up-and-down movements of small amplitude, including some in which a negative velocity transient was accompanied by high positive pitch, indicating that the squid was descending arms-first (down arrows and diagrams), as opposed to the usual fins-first direction. All of the sudden vertical movements shown

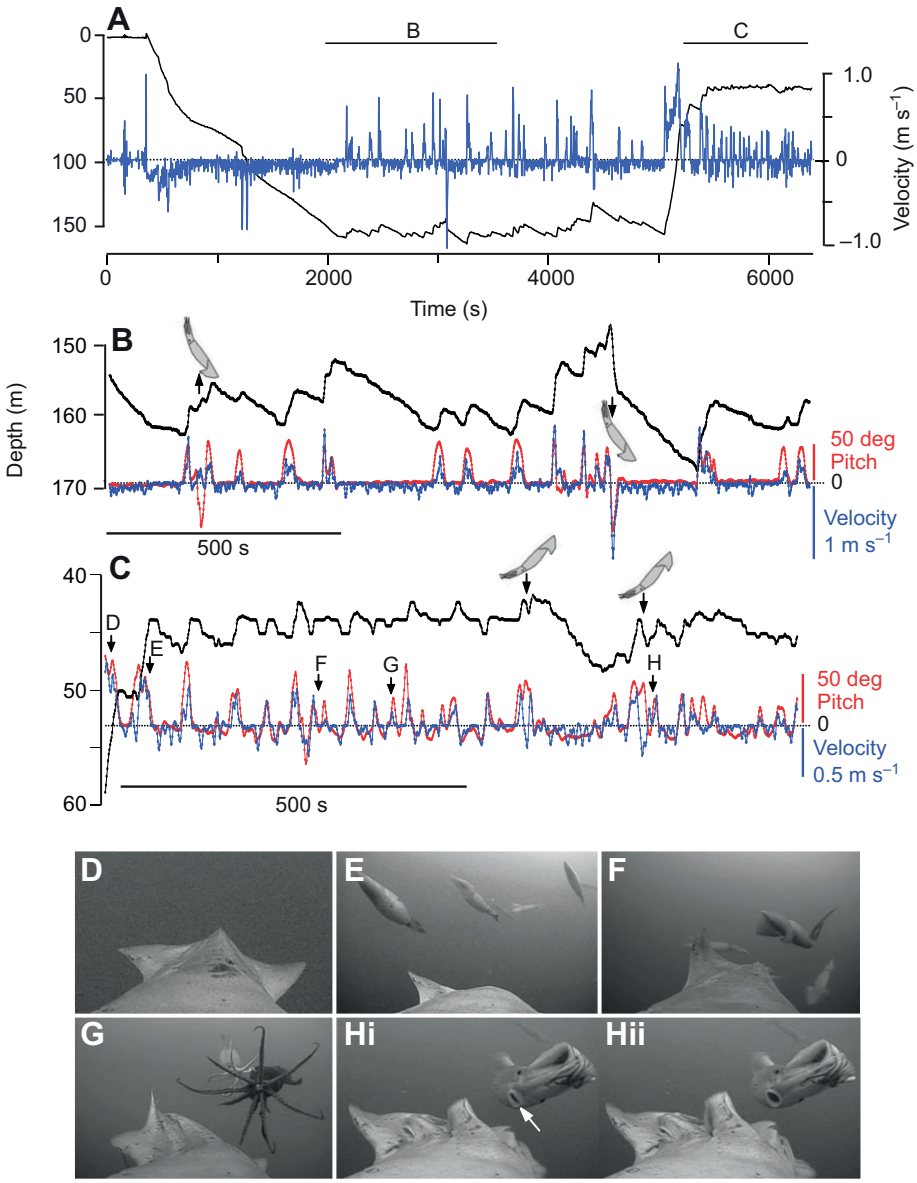

Fig. 5. Depth-maintenance behavior of *Dosidicus gigas*. (A) Complete depth (black) and velocity (blue) records for AVP deployment 3. Segments labeled B and C are displayed at higher resolution in panels B and C. (B) Typical depth-maintenance behavior involving climb-and-glide swimming that is occasionally interrupted by other movements. Black trace is depth, blue is velocity and red is pitch. The diagrammed squid on the left represents an arms-first ascent with a negative pitch (fins down), presumably with the siphon directed in the posterior direction. A rapid fins-first descent is diagrammed on the right. (C) Tight depth-maintenance with numerous rapid up-and-down motions and little gliding. Several downwards jets are carried out at positive pitch, indicating that the squid was descending arms-first (down arrows and diagrams). Labels with arrows indicate times of the video frames displayed in panels D–H during which the squid interacted with conspecifics. (D) Dorsal surface of the head and arms of the AVP-carrying squid. The arms are held closely together, and the fin-like structures are the prominent lateral keels on the third arm from the dorsal midline. (E) A group of conspecifics. The bright area in upper right is sunlight at the surface. (F) An approaching squid swimming ventral-side up. (G) Two approaching squid with outstretched arms. (H) Sequential frames (58.8 ms interval at 17 Hz) of an approaching squid showing a large change in siphon diameter (arrow).

in Fig. 5C were probably associated with a close encounter with a conspecific, and a sampling of video frames captured is shown in Fig. 5D–H. Interactions included displays involving arm posture and apparent mating attempts, as evidenced by the appearance of spermatophores between the arms of the AVP-bearing squid (presumably a female based on its large size). Close interactions of this sort were always accompanied by chromatophore displays, and these behaviors will be described in detail in a subsequent publication.

Two features evident in the video frames are relevant to swimming mechanics. First, the arms are generally held tightly together and pointed in the anterior direction (Fig. 5D), with the prominent lateral keels on the third arm from the dorsal midline held in a position that resembles the posterior fins. Presumably this posture of the arms, like the fins, provides a stabilizing influence, but there was no indication of movement of the arms in a way that would generate propulsive thrust. Second, the siphon (arrow in Fig. 5Hi) is capable of large and rapid diameter changes (58.8 ms between sequential frames in Fig. 5Hi,Hii). This ability would provide an additional and highly effective control element for jet velocity.

Vertical distribution, environmental features and behavior

Daytime vertical distribution and oxygen concentration

Examples for tags deployed in autumn, spring and summer are shown in Fig. 6, and summary data for all PAT tags over the initial 3 days of deployment are provided in Table 2. Regardless of the time of year, all tagged squid spent daytime hours primarily at an average depth of 200–250 m where temperature was ~13°C. Oxygen concentration at these depths ranged from 12 to 70 μmol kg^{-1} (Table 2). Tags deployed off Santa Rosalia in the autumn (10/04 and 11/08A, B) showed median daytime depths where oxygen concentration was characteristic of the upper OMZ (≤20 μmol kg^{-1}). Springtime deployments revealed a more variable picture, with oxygen at daytime depths ranging from 12 μmol kg^{-1} (Guaymas, 03/07A) to ~60 μmol kg^{-1} (Guaymas, 03/07B and Santa Rosalia, 05/08). Corresponding summertime values from San Pedro Martir were also ~60 μmol kg^{-1} (07/06A, B). Although this upper range of oxygen concentration is higher than that found in the OMZ proper, it is low enough to be considered hypoxic for many pelagic fish (Diaz and Rosenberg, 1995; Hofmann et al., 2011).

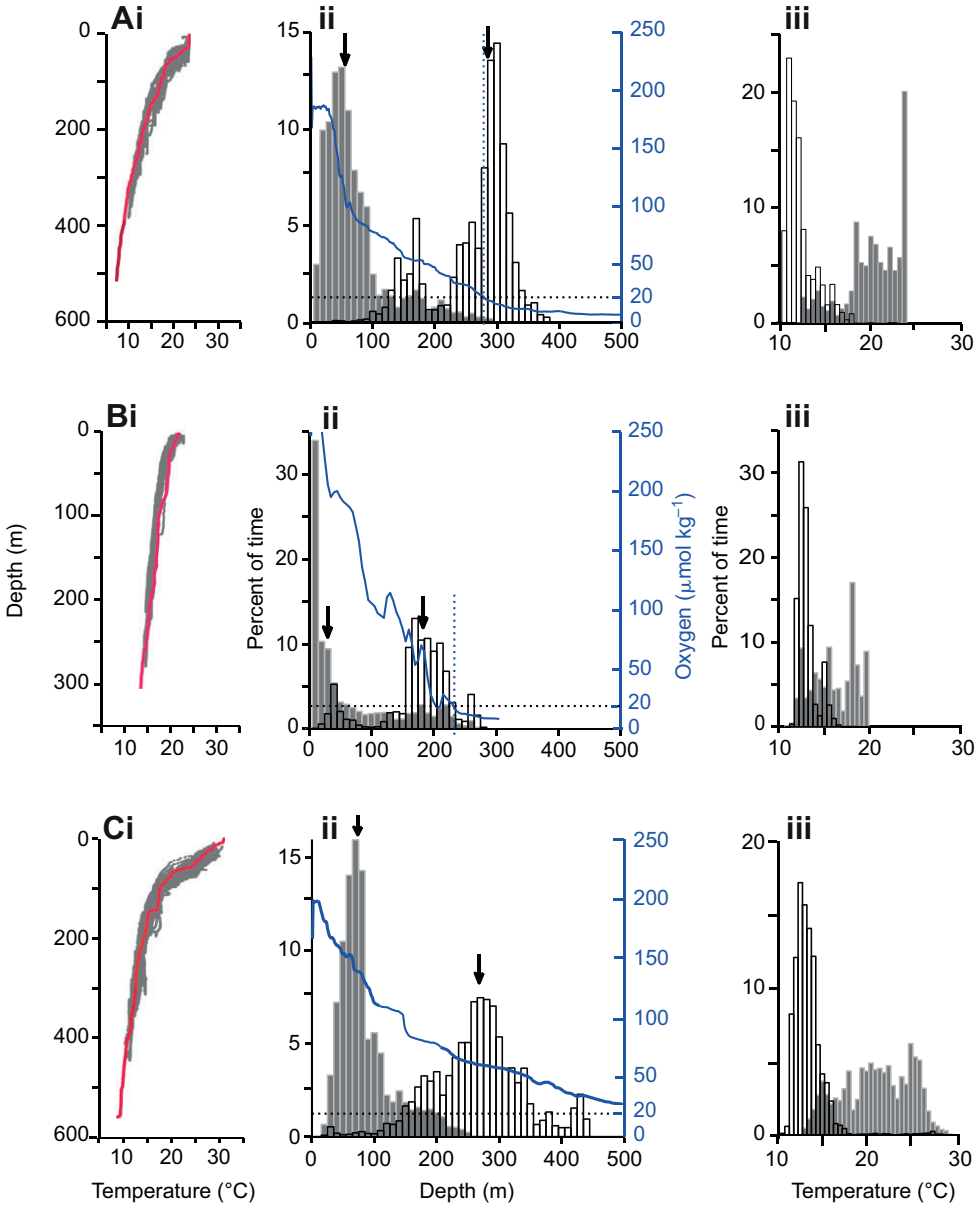

Fig. 6. Summary data for PAT tags during the first 3 days of deployment on *Dosidicus gigas* in different seasons (same tags as Fig. 2). (A) Tag 11/08B in autumn. (i) Temperature–depth profiles at the site of tag deployment determined by CTD cast (solid red trace) and by the tagged squid (gray points). These data are consistent with the squid remaining in a body of water with fairly uniform properties during the first 3 days. (ii) Time-at-depth histograms for nighttime (local sunset to sunrise, gray bars) and daytime (open bars). Arrows indicate depth at median values. Solid blue trace represents oxygen concentration as determined by CTD cast at the site of tag deployment. Horizontal dotted line indicates the upper boundary of the OMZ; vertical dotted line indicates the depth of the OMZ. (iii) Time-at-temperature histograms for nighttime (gray bars) and daytime (open bars). (B) Tag 03/07B in spring. The depth axis has been truncated at 500 m; contribution by a single deep dive is negligible (see Fig. 2B). (C) Tag 07/06B in summer. The depth axis has been truncated at 500 m; contribution by a single deep dive is negligible (see Fig. 2C). Data in B and C are presented in the same format as for A.

In three cases, hydrographic properties were surveyed over a sizeable region to reveal the variation of oxygen at depth around the sites of each tag deployment (Fig. 7A). Oxygen (Fig. 7B) and temperature profiles (not shown) in the Santa Rosalia region in November 2008 revealed spatial variation in the thickness of the surface mixed layer (upper 75 m), but depths of the contours for both 20 and 60 μmol kg^{-1} oxygen were quite constant over the area surveyed (Fig. 7C). More variation in oxygen at midwater depths occurred off Guaymas in March 2007, but the 20 μmol kg^{-1} oxygen contour was again fairly constant (Fig. 7D). These results are consistent with the idea that some squid tagged in these areas in spring and autumn spent considerable time in the upper OMZ (Fig. 2A,B, Table 2) as well as in the less hypoxic, shallower region (20–60 μmol kg^{-1} oxygen) that we will call the oxygen limited zone (OLZ).

Summer deployments in the San Pedro Martir Basin present a fundamentally different case. In this region the upper boundary of the OMZ is considerably deeper than in the areas discussed above (Fig. 7E). Depth of the OMZ generally increases with latitude in the Gulf of California and never falls to OMZ levels north of the shallow sill separating the Guaymas Basin from the Midriff Islands [yellow herringbone line in Fig. 1; see also fig. 2 in Alvarez-Borrego and Lara-Lara (Alvarez-Borrego and Lara-Lara, 1991)]. These features are consistent with the high daytime oxygen concentrations observed for squid in this area (tags 07/06A,B; Table 2) at a 'normal' daytime median depth of ~250 m. Time-series data in Fig. 2C suggest that this squid entered the OMZ only once (deep dive on 08/02) during the entire 21-day deployment, because the pop-up location of the tag was well north of the sill.

Comparison of the median daytime depth of tagged squid with depth of the upper boundary for the OMZ (Fig. 7F) shows that these parameters are very similar in some cases, but not in others. Points for all autumn tags (Santa Rosalia) and one spring tag from Guaymas (03/07A) lie on or slightly above the dotted line of unity slope, whereas the other spring (03/07B and 05/08) and both summer tags (07/06B,C) do not. Daytime depths for these squid are all shallower than the local OMZ depth, and in the case of the San Pedro Martir tags the difference is extreme. Nonetheless, median

Table 2. Characteristic depth, temperature and oxygen concentration of habitats occupied by tagged Humboldt squid

	CTD				Tag – Night			Tag – Day		
Month/Year (Tag ID)	Date	Latitude (°N)	Longitude (°W)	OMZ depth (m)	Temperature (°C)	Depth (m)	Oxygen (μmol kg^{-1})	Temperature (°C)	Depth (m)	Oxygen (μmol kg^{-1})
10/04 (52869)	10/15/04	27.32	112.17	214	18.7±3.7 [18.7]	113±77 [91]	66	14.5±2.0 [14.1]	210±66 [212]	21
07/06B (64006)	07/18/06	28.45	112.53	559	20.9±3.9 [21.0]	88±46 [74]	132	13.5±1.9 [13.2]	266±74 [269]	61
07/06C (60970)	07/18/06	28.45	112.53	559	20.5±3.1 [21]	80±33 [72]	140	14.0±1.3 [14]	239±45 [248]	63
03/07A (62007)	03/15/07	27.93	111.28	230	16.9±2.6 [16.8]	65±78 [36]	193	13.1±2.3 [12.1]	218±94 [255]	12
03/07B (62009)	03/15/07	27.93	111.28	230	15.9±2.2 [15.8]	70±74 [32]	204	13.1±1.0 [12.9]	172±57 [182]	50
05/08 (64006)	05/05/08	27.34	112.12	376	16.6±2.1 [16.6]	53±57 [33]	218	12.2±1.0 [12.0]	255±58 [264]	70
11/08A (64004)	11/17/08	27.51	112.28	282	19.6±2.1 [19.6]	56±37 [53]	98	12.2±2.3 [11.5]	253±72 [282]	18
11/08B (83048)	11/17/08	27.51	112.28	282	19.3±2.8 [19.6]	74±54 [60]	100	12.3±1.6 [11.7]	261±62 [285]	17
Average					18.6 [18.7]	74.9 [56.4]	143±56	13.1 [12.7]	234.2 [249.6]	39±24

Oxygen data were obtained close as possible (in space and time) to match tag deployment. Oxygen minimum zone (OMZ) depth is that where oxygen concentration is 20 μmol kg^{-1}. Temperature and depth tag data (mean ± s.d. [median]) were computed for the first 3 days of tag deployment in the same area where oxygen profiles were measured, except for tag 11/08A. This squid made a deep dive to 1342 m for ~6 h on day 2, and days 3–5 were used for purposes of this table as justified by CTD casts made over the likely path followed by this squid (based on endpoint, see Fig. 1 and Fig. 7A). Oxygen concentrations tabulated are values at the median nighttime or daytime depth from each tag. Oxygen data from October 2004 were not available, and measurements from early November 2005 were substituted. Average data represent the overall mean and median (brackets) of individual tags.

daytime depth of all these tags would be classified as generally hypoxic by the 60 μmol kg^{-1} criterion that we use to define the OLZ.

Nighttime vertical distribution and temperature

Overall, tagged squid spent nighttime at a median depth of ~60 m and a temperature of 19°C, a region with high oxygen concentration (~145 μmol kg^{-1}) (Table 2). Sizeable differences between individual squid in median nighttime depths and temperature reflect the strong seasonal variation in surface temperature in the Gulf of California. Lowest median nighttime temperatures and shallowest depths occupied by squid occur in spring (03/07A,B and 05/08) when surface temperatures are cool (Table 2, Fig. 8A), and highest temperatures and greatest depths occur during summer when surface temperatures reach a maximum.

From early summer through late autumn, surface temperatures in the Guaymas Basin exceed 25°C, but the squids' median nighttime temperature never exceeded 21°C (Fig. 8A), suggesting a potential thermal limit near this value. This idea is consistent with the amount of time individual squid spent exploring the upper 10 m of the water column in different seasons (Fig. 8B). Mean temperature in this depth zone was cool in spring, and the average duration of an excursion was ~3 h, with some lasting over 6 h. In summer, when surface waters were nearly 30°C, the longest excursion was <10 s. Occupancy of the upper 10 m also tended to be low in autumn, when temperature generally exceeded the thermal limit suggested above. Only one excursion lasting longer than 37 min was observed at temperatures greater than 21°C (7.7 h at 22.1°C).

Vertical distribution and light

PAT tags used in our study have a sensitive light sensor that permits a relative measure of illumination on a logarithmic scale. Fig. 9 (left panels) shows complete depth (upper, blue) and light (lower, gray) records for the tags discussed in conjunction with Figs 2 and 6. Arrows in each panel indicate the day on which the tag detached from the squid and began floating at the surface, with maxima and minima after this time representing day and night, respectively. Panels on the right show the distributions of time spent at different light levels for the tagged squid and floating tag. In general, light levels recorded by the tagged squid during both day and night are similar, and both are substantially lower than the light level at the surface at night. Variability in nighttime light levels for floating tags reflects the lunar phase; a transition from full moon on 9 August 2006 to new moon on 23 August 2006 is evident in Fig. 9Ci. All tags analyzed in this paper showed similar patterns for day and night light levels.

Although the tagged squid spent the vast majority of their time under conditions of extremely dim light, vertical excursions to levels of illumination characteristic of daylight are evident for each data set in Fig. 9. These excursions tend to be brief (Fig. 9Ai) and often occur over several sequential days (Fig. 9Bi,Ci). During these times, high-frequency vertical movements can obscure the regular diel pattern; this is most obvious in the data shown in Fig. 9Ci. This behavioral pattern is seen during both cold (March; Fig. 9Bi) and hot (July, Fig. 9Ci) seasons, and it occurs during daytime as well as nighttime (compare Fig. 9Bi,Ci with Fig. 2B,C).

Effects of OMZ conditions on vertical velocity

Four tagged squid (03/07A,B and 11/08A,B) spent time in the upper OMZ (Fig. 2, Table 2) in an area where we made extensive oxygen surveys before and after tagging (Fig. 7). Vertical velocity distributions from these tags were analyzed for three specific depth zones, each 100 m thick, that are relevant to the effects of hypoxia on swimming performance: (1) the well-oxygenated 'surface' layer (0–100 m depth); (2) the seriously hypoxic 'OMZ' (100 m layer immediately below the 20 μmol kg^{-1} oxygen contour); and a 100 m layer just above the OMZ that roughly corresponds to the OLZ (20–60 μmol kg^{-1} oxygen; see Fig. 7C,D). Overall velocity distributions for these three zones are plotted in Fig. 10A. Ratios calculated for OMZ and OLZ values relative to the surface zone are plotted in Fig. 10B.

Vertical velocity can be divided into three categories (see Fig. 10A) based on comparisons between the velocity distributions for different depth zones: low (–0.1 to +0.3 m s^{-1}), intermediate (up to ±1 m s^{-1}) and high (>±1 m s^{-1}). Fractions of time spent in the low velocity range are similar across the three depth zones, and in each case this range accounts for >90% of the total distribution. These low velocities are associated with the most gentle vertical movements, including passive sinking, which alone accounts for 80% of the total time (–0.15 to +0.05 m s^{-1}).

Fractions for positive intermediate velocities are comparable in the surface zone and the OLZ, but OMZ fractions are approximately half of these (Fig. 10B). Negative velocities in the intermediate range tend to be greatest in the OLZ, although there is some variability (Fig. 10B). OMZ fractions are again reduced in this region relative to both of the

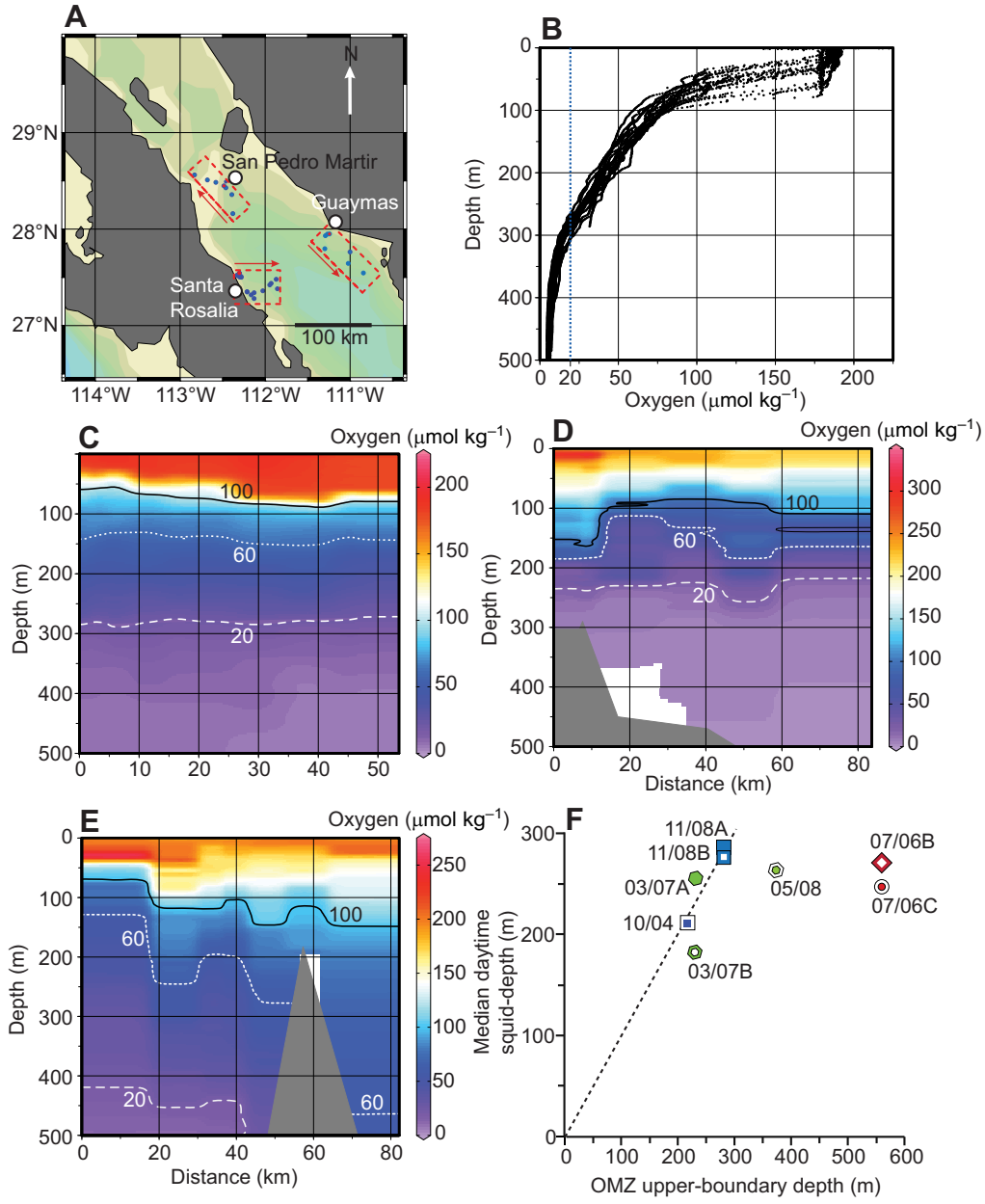

Fig. 7. Oxygen at depth in the areas of PAT tag deployments on *Dosidicus gigas*. (A) CTD casts were made at the sites indicated by small blue circles inside the dashed boxes for each tagging region: Santa Rosalia (autumn, tags 11/08A,B), Guaymas (spring, tags 03/07A,B) and San Pedro Martir (summer, tags 07/06B,C). Direction of the arrows corresponds to that of transects plotted in panels C–E, with the base of the arrow at a distance of 0 km in each case. (B) Oxygen profiles for all casts in the Santa Rosalia region made between 12 and 19 November 2008. (C) Oxygen at depth along the Santa Rosalia transect. Contours are plotted for oxygen at 20 μmol kg^{-1} (dashed white), 60 μmol kg^{-1} (dotted white) and 100 μmol kg^{-1} (solid black). Casts corresponding to the cluster of points at the tag-deployment site (northwest corner of box in A) were made on 16–17 November. Tags were deployed on 16 November. (D) Oxygen at depth along the Guaymas transect. CTD casts were made in the area of tag deployment (cluster closest to Guaymas in A) on 17–20 March 2007. The transect was completed on 1 April following tag recovery. Oxygen contours are labeled as in C. (E) Oxygen at depth along the San Pedro Martir transect (southeast to northwest). CTD casts were made to the northwest of the island on 17–18 July 2006, and tags were deployed in this region. The two casts south of the island were made on 20–21 July. Oxygen contours are labeled as in C. (F) Relationship of median daytime depth of squid as determined by PAT tags with the upper boundary of the OMZ (20 μmol kg^{-1} oxygen). The dashed line has a slope of 1. Green symbols represent tags deployed in spring, red those deployed in summer and blue those deployed in autumn.

other layers. Thus, vertical movements in this intermediate velocity range are substantially slowed in the OMZ. This velocity range accounts for 7.2% of the total time in the surface zone, 9.3% in OLZ and 4.1% in OMZ. Together, the low and intermediate velocity ranges account for >99% of all time spent in each zone.

Maximum velocities in the surface zone were –2 and +2.7 m s^{-1}, and the total range of velocities was progressively reduced in the other zones: –1.8 to +2.0 m s^{-1} in the OLZ and –1.2 to +1.7 m s^{-1} in the OMZ (Fig. 10A). Direct comparison of fractions of time spent at high velocities across depth zones is not straightforward, because these events are extremely rare and account for <0.02% of the total time. In order to assess higher velocities in another way, we counted the number of times each tagged squid exceeded a certain velocity threshold, regardless of how long the squid remained above that threshold. This provides a number of discrete 'events' when velocity exceeded the threshold value. Fewer than 10 events in each depth zone are responsible for all velocities exceeding –1.0 or +1.5 m s^{-1} (Fig. 10C), and the relative number of high-velocity events is reduced in the OMZ, particularly for negative velocities. This approach is also informative about intermediate velocities. It is evident from inspection that the number of events (Fig. 10D) associated with the intermediate velocity range in the upper OMZ is also generally approximately half of the corresponding values in the OLZ or surface zones. This pattern is similar to that discussed in conjunction with Fig. 10B.

Vertical velocities during depth-maintenance behavior in all depth zones analyzed were confined to the low and intermediate ranges (Fig. 10E). Total time spent in depth-maintenance behavior in the surface zone was 16%, and values in the OLZ and OMZ were 5 and 20%, respectively. This range is similar to that computed for all depth maintenance during an entire deployment (3.4–18.5%). Velocities in the intermediate range associated with this behavior were greatly diminished in the OMZ and less so in the OLZ (Fig. 10F). The greater reduction of intermediate velocities in the OMZ *versus* OLZ is thus qualitatively similar to the pattern described above for overall jetting performance.

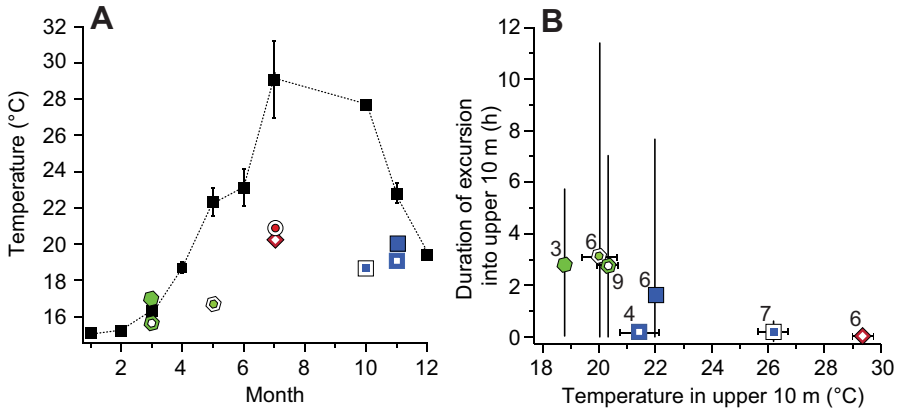

Fig. 8. Lack of occupancy of temperatures above 21–22°C. (A) Seasonal change in sea surface temperature and median nighttime temperatures occupied by PAT-tagged *Dosidicus gigas*. Sea surface temperatures (black squares, means ± s.d.) were recorded in the Santa Rosalia area and are representative of the Guaymas Basin. Symbols for individual tags are the same as in Fig. 7F. Median nighttime temperature never exceeded 21°C. (B) Duration of excursions by PAT-tagged squid into the upper 10 m of the water column decreases during warm summer and autumn months (same tag symbols as in A). Plotted values are means, and vertical lines indicate ranges. Temperature error bars represent ±1 s.e.m.

DISCUSSION

Previous studies have indicated that *D. gigas* spends considerable time at cold, hypoxic depths, both in the Gulf of California (Gilly et al., 2006) and in the Pacific Ocean (Bazzino et al., 2010; Zeidberg and Robison, 2007). This paper provides an expanded and refined assessment of this feature by exploring squid swimming behavior in the Guaymas Basin of the Gulf of California in locations that are characterized by large seasonal differences in surface temperature and depth of the upper boundary of the OMZ. This paper also presents the first data using an AVP with squid and provides insight into the basic patterns of jet-propelled locomotion *in vivo* from an oceanic squid, a group that has not been previously examined from

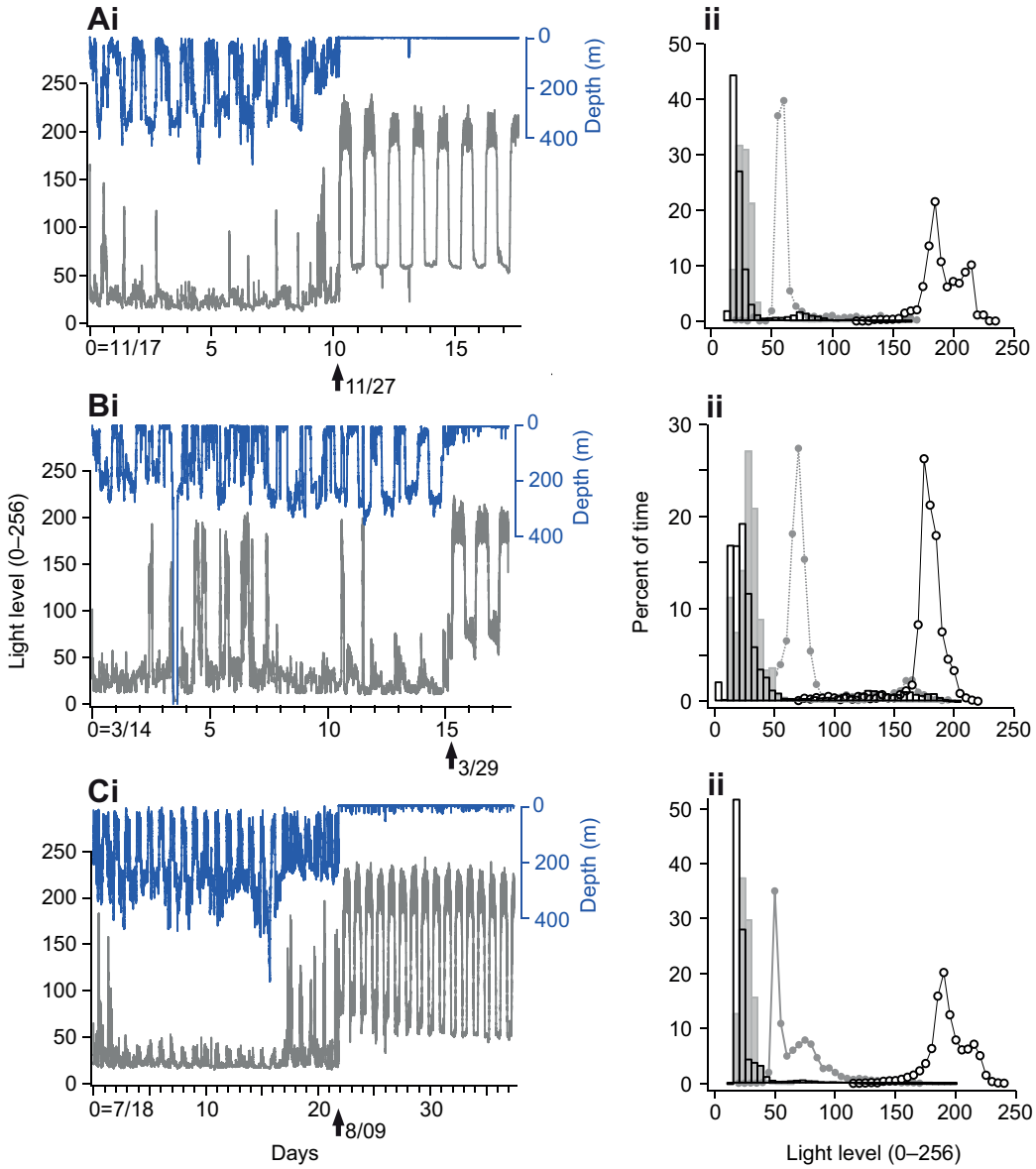

Fig. 9. Light sampled by tagged *Dosidicus gigas*. The left panels (Ai–Ci) show depth (blue, upper trace) and ambient light in units as assigned by the tag (gray, lower trace) for the same tags as in Fig. 3 (A=11/08B, B=03/08B and C=07/06B). The light-level scale is logarithmic. The light sensor is located on the body of the tag 1.5 cm beneath the float. In each case, the arrow indicates when the tag ascended to the surface after detaching from the squid (mm/dd). Right panels (Aii–Cii) show the distributions of time spent at each light level. Bars represent data collected when the tag was attached to the squid (solid, nighttime; open, daytime). Circles represent data collected by the tag as it floated on the surface (gray, nighttime; open, daytime).

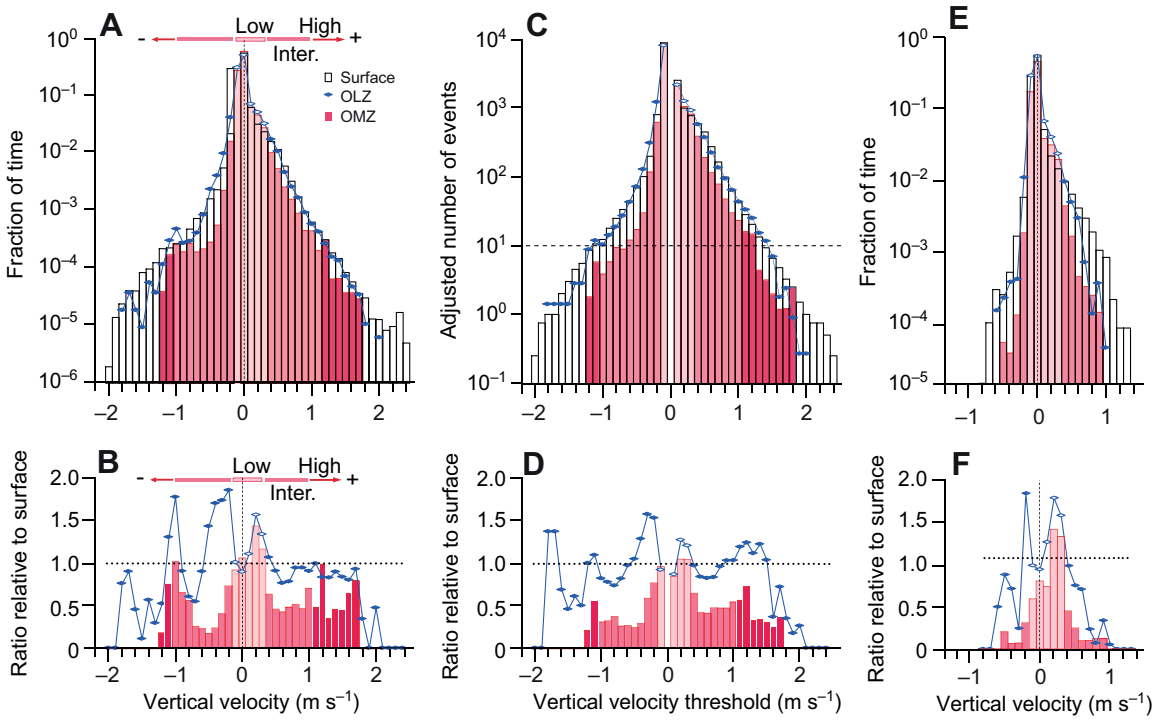

Fig. 10. Reduction of vertical velocities of *Dosidicus gigas* at hypoxic depths. Data from the first 3 days of PAT tag deployments (tags 03/07A,B and 11/08A,B; see legend to Table 2) were analyzed for three 100 m layers in the water column: surface (open bars; upper 100 m), oxygen limited zone (OLZ) (symbols; directly above the 20 μmol kg^{-1} oxygen contour) and oxygen minimum zone (OMZ) (shaded bars; immediately below the 20 μmol kg^{-1} oxygen contour). Ranges for low, intermediate and high velocity are indicated at the top of A and B and are coded in all panels by the shading (the lightest shading represents the lowest velocities). (A) Vertical velocity distributions (means in 0.1 m s^{-1} velocity bins) for surface, OLZ and OMZ layers, each normalized to the total number of points in that depth zone: surface (03/07A=127,688, 03/07B=110,524, 11/08A=64,004, 11/08B=118,830); OLZ (03/07A=26,811, 03/07B=123,362, 11/08A=50,628, 11/08B=41,338); OMZ (03/07A=93,420, 03/07B=14,908, 11/08A=88,807, 11/08B=61,400). (B) Ratios of fractions in A for OMZ and OLZ relative to the surface layer (the horizontal dotted line indicates the range of surface values). (C) Distribution of the mean number of vertical excursions (events) exceeding a given threshold for all vertical velocities (0.1 m s^{-1} bins) >0.05 m s^{-1} and <–0.05 m s^{-1} in OMZ, OLZ and surface layers. Plotted values for the surface layer are raw counts. Adjusted numbers for OMZ and OLZ were computed for each tag by normalizing the raw counts in each velocity bin by the ratio of the total time spent in the specific depth zone to the total time spent in the surface zone as follows: OMZ (03/07A=1.64, 03/07B=8.73, 11/08A=1.14, 11/08B=1.58) and OLZ (03/07A=5.48, 03/07B=1.05, 11/08A=1.99, 11/08B=2.42). (D) Ratios of values plotted in B for OMZ and OLZ relative to the surface layer (dotted line). (E) Vertical velocity distributions for depth-maintenance behavior in the OMZ, OLZ and surface layers. Total number of points for each depth zone: surface (03/07A=35,173, 03/07B=8406, 11/08A=16,577, 11/08B=11,062); OLZ (03/07A=30,165, 03/07B=3260, 11/08A=5407, 11/08B=1005); OMZ (03/07A=31,330, 03/07B=0, 11/08A=7043, 11/08B=13,571). (F) Ratio of values plotted in E for OMZ and OLZ relative to the surface layer (dotted line).

this point of view. These insights into swimming behavior provide a foundation for evaluation of the effects of hypoxia on performance.

Climb-and-glide locomotion and vertical velocity ranges

Data from both AVP and PAT-tag deployments are consistent with the idea that nearly all locomotor behavior of *D. gigas* is carried out through climb-and-glide swimming. Temporal summation of elemental climb-and-glide events underlies a rich assortment of vertical movements, and the strength of an elemental jetting event (as defined by its time course) can also vary. Neural mechanisms for control of jetting strength in *D. gigas* are presumably similar to those in a loliginid species, where jets of similar time course can vary over a large amplitude range depending on the motor pathway recruited and the intensity of neural activity (Otis and Gilly, 1990; Gilly et al., 1996). Another mechanism for varying the strength of individual jets in *D. gigas* would be active control of siphon diameter (Fig. 7H), but we cannot quantify siphon dynamics in free-swimming squid at present.

Gliding appears to account for the vast majority of a squid's time. Over 80% of the total time with PAT tags was spent at vertical velocities of –0.15 to +0.05 m s^{-1}, a range that includes passive sinking (Fig. 10A). Clearly, the vast majority of a squid's time is spent ascending slowly, presumably with weak jetting and fin beating, and descending even more slowly by gliding.

Based on the simple model for climb-and-glide swimming presented, Eqn 4 predicts a net horizontal velocity during passive gliding of ~0.25 m s^{-1}, and the total amount of time spent in the above velocity range would correspond to a total horizontal motion of ~22 km day^{-1}. This value is comparable to a figure of 30 km day^{-1} estimated for *D. gigas* based on PAT tag deployments (Gilly et al., 2006) and is consistent with estimates of maintained horizontal speed during long-distance migrations of other oceanic squids (Dawe et al., 1981; Nakamura, 1993; O'Dor et al., 1994; Yatsu et al., 1999; Yano et al., 2000; Stark et al., 2005). Thus, it appears that *D. gigas* may generate a substantial fraction of total horizontal movement through passive gliding. Obviously weak horizontally directed jetting or fin activity during gliding could greatly extend total horizontal movement.

Virtually all of the additional 20% of a squid's time is spent actively ascending and descending at intermediate velocities of <1 m s^{-1} magnitude. These motions can be quite complex, but are essentially composed of temporal summation of individual jetting

events of varying strength and frequency. Because climb-and-glide swimming is also involved in these more active motions, it is likely to be an important component of most behaviors.

Fast vertical movements of >1 m s^{-1} are extremely rare (Fig. 10C), accounting for only 0.2% of time in the upper 100 m and even less in the other depth zones analyzed (Fig. 10A,C). Maximum vertical velocities can exceed 3 m s^{-1} (data not shown, but see Fig. 10A), but the functional importance of these rare and brief events is not known. Recent measurements using active acoustics (5–10 Hz sampling) of free-swimming *D. gigas* engaged in coordinated, nighttime foraging behavior have revealed short bursts (<1 s) of activity with vertical velocities approaching 4 m s^{-1} and horizontal velocities of nearly 30 m s^{-1} (Benoit-Bird and Gilly, 2012). Such high burst speeds are comparable to the fastest teleost fishes, but it is highly unlikely that they could be maintained by a squid for very long.

Climb-and-glide and efficiency of jetting

Metabolic rates of swimming squid, mostly loliginids, have been estimated in flumes (O'Dor and Webber, 1986; O'Dor et al., 1994; Bartol et al., 2001a; Bartol et al., 2001b), and such studies have confirmed that swimming by jet propulsion is much less efficient than tail-beating in fish (O'Dor, 1982; O'Dor, 1988; O'Dor, 2002; Webber et al., 2000). A large fraction (30–90%) of a squid's total energy expenditure in a flume is spent in maintaining horizontal position, and if climb-and-glide swimming were possible, a correspondingly large energy savings might be realized (O'Dor, 1988). Because passive sinking (gliding) accounts for ~80% of total time of a tagged squid in the natural oceanic setting, it is clear that climb-and-glide behavior by free-swimming *D. gigas* must indeed save a great deal of energy compared with horizontal swimming against a current in a physically constraining flume.

Flow-tank studies of active swimming by an oceanic squid such as *D. gigas* are therefore likely to overestimate metabolic demands to achieve a given horizontal velocity in an ecologically relevant context. If climb-and-glide locomotion were possible in such studies, the overall efficiency of jet-propelled swimming of a large Humboldt squid would probably be much closer to that of comparably sized teleosts than previously thought. Use of the fins by *D. gigas* in swimming would also tend to increase efficiency. But negatively buoyant, oceanic fish such as yellowfin tuna also employ climb-and-glide swimming (Schaefer et al., 2007), so locomotion *in vivo* for such teleosts would probably still be more efficient.

Depth-maintenance behavior

Depth maintenance (defined here as holding depth within a range of ±15 m for a period of ≥15 min) accounted for up to 20% of the total time at liberty for squid carrying PAT tags. This behavior generally involved simple patterns of climb-and-glide swimming and was always restricted to the low and intermediate vertical velocities that account for over 99% of the total time spent in locomotion.

It seems likely that depth maintenance is a generic pattern of activity that is expressed at a particular time and place when the context warrants careful attention of a specific region of the water column. One context is engagement in a variety of social interactions with conspecifics (Fig. 5), including mating. Another likely function would be foraging on patches of densely compacted micronekton, which can occur anywhere in the water column. Once such a rich resource was located, it is likely that a particular depth suitable for exploitation would be focused on through repetitive, small-amplitude climb-and-glide events.

Environmental factors and daytime habitat for squid: oxygen and light

Low oxygen concentrations found in the upper OMZ (<20 μmol kg^{-1}) have been proposed to limit the daytime depth occupied by *D. gigas* (Gilly et al., 2006; Rosa and Seibel, 2010), and data presented in this paper are to some extent consistent with this position. Comparison of the vertical distribution of squid determined with PAT tags with extensive hydrographic surveys in the areas of tag deployment indicate that daytime habitat (defined by median daytime depth) can correspond closely to the upper boundary of the OMZ in Santa Rosalia in autumn and Guaymas in spring (Fig. 7F). But in other locations and seasons this relationship breaks down, indicating that oxygen concentration is not the only relevant factor that determines preferred daytime habitat.

Decoupling of daytime habitat from the upper OMZ occurs in at least two ways. First, the OMZ can be substantially deeper than 250 m, either due to location (San Pedro Martir, tags 07/06B,C) or season (spring, tag 05/08), resulting in a daytime depth for squid at shallower depths and higher oxygen concentrations. Second, an individual squid may spend an unusually large fraction of time at shallow depths during the day, again yielding a median daytime depth that is shallower than the OMZ. This situation was observed in Guaymas (tag 03/07B) during spring when the upper water column was much cooler and had a higher oxygen concentration than in the autumn (Fig. 6A,B). These observations indicate that an association with the upper OMZ is not obligatory for large, adult squid, at least on a time scale of days to weeks.

Light is also a contributing factor to the daytime depth of squid. All tagged squid spent most of their time, both day and night, at depths that are darker than a moonless night at the sea surface. Diel vertical migration (Figs 2, 9) is clearly a relevant behavioral mechanism, but it is doubtful that light directly sets the vertical distribution of *D. gigas*. Numerous transient excursions to much brighter depths occur during both day and night, indicating that squid explore a variety of light levels. But light is likely to be a critical factor in determining the vertical distribution of the mesopelagic micronekton (fish, molluscs and crustaceans) of the DSL (Boden and Campa, 1967) on which *D. gigas* preys (Markaida et al., 2008). We hypothesize that *D. gigas* can forage on these organisms at depth during daytime, and that the vertical distribution of these prey organisms is the primary driver of the distribution of *D. gigas*.

In autumn and spring in the Guaymas Basin, the depths of the DSL and the upper OMZ boundary often both occur at ~250 m (K. Benoit-Bird, personal communication), and this depth would then set the daytime depth of *D. gigas*. When the OMZ is much deeper than 250 m, as discussed above, we hypothesize that DSL organisms on which *D. gigas* preys also decouple from the OMZ and remain at their preferred light level at 250–300 m, along with the squid that can utilize the DSL as a daytime foraging ground.

We have not seen a case in the Guaymas Basin where the OMZ is significantly shallower than the median daytime depth of squid as documented in this study (200–250 m; Table 2). In the southern Gulf of California (below ~25.5°S) the upper boundary of the OMZ can be much shallower (Alvarez-Borrego and Lara-Lara, 1991) (W.F.G., unpublished data), but tag data from this area are not available. If a shallow OMZ does present a limit to daytime depth at certain places and times, it is not entirely clear whether the directly impacted species would be *D. gigas* or some members of the DSL community on which *D. gigas* forages. Acoustic studies to simultaneously quantify vertical distributions of both the DSL and squid in conjunction with spatial or seasonal

variation in OMZ depth, along with biochemical and physiological studies on both squid and their prey species would clarify this issue.

Temperature and nighttime habitat for squid

Aversion of adult *D. gigas* to temperatures of >22°C was previously proposed based on an analysis of diving dynamics (Davis et al., 2007). Tagging data from the present study support this idea and suggest an upper thermal limit of 21–22°C for median nighttime depth of *D. gigas* (Fig. 8A). When surface temperatures are cooler than this limit, considerable time is spent at shallow depths, with excursions into the upper 10 m of water column lasting up to 12 h (Fig. 8B). But very little time is spent there when the surface temperature exceeds this limit, and excursions are extremely brief. These observations are consistent with opportunistic foraging on small epipelagic fishes such as anchovies when surface temperatures are permissive in spring (Markaida et al., 2008), and brief forays into warm surface waters are also probably related to foraging. Physiological limitations are likely to underlie these observations, because the temperature dependence of resting metabolic rate in this thermal range is extremely high (Rosa and Seibel, 2008; Rosa and Seibel, 2010).

Effects of OMZ conditions on performance

Tagged squid can spend a substantial amount of time, primarily during daytime, moving in and out of the upper OMZ (Fig. 2A,B). We hypothesize that foraging on myctophids and other DSL organisms can occur during these times. Maintained activity under hypoxic conditions raises some questions, because laboratory studies of *D. gigas* have revealed a large suppression (>80%) of resting aerobic metabolic activity under temperature and oxygen conditions that mimic those of the upper OMZ (Gilly et al., 2006; Rosa and Seibel, 2008). *Dosidicus gigas* has not been studied swimming under OMZ conditions in the laboratory, but fast swimming for any substantial period of time would almost certainly be greatly impaired (Rosa and Seibel, 2010).

Vertical velocity in the field provides an indicator of performance that can be used to assess the effects of cold temperatures and hypoxia as found within the OMZ. Results in this study indicate that low-velocity movements ($-0.1\,m\,s^{-1}$ to $+0.3\,m\,s^{-1}$) are not impacted by OMZ conditions, but ascending and descending velocities in the intermediate range (Fig. 10A,B) are reduced by ~50% in the upper OMZ relative to both of the shallower zones analyzed (OLZ and oxygenated surface). Maximum observed velocities and the number of high-velocity events ($>1\,m\,s^{-1}$ magnitude) are reduced even more severely in the upper OMZ (Fig. 10C,D). Oxygen is likely to be the limiting factor underlying the diminished vertical velocities in the OMZ relative to the OLZ, because the temperature differential between these layers is rather small.

Intermediate vertical velocities during depth-maintenance behavior are reduced to an even greater extent in the upper OMZ relative to the surface zone (Fig. 10E,F). A similar but less marked effect is evident for the OLZ. Whether depth maintenance serves the same functional roles in the different depth zones is unknown, but it is clear that velocities of $>0.5\,m\,s^{-1}$ associated with this behavior are slowed down by at least 80% in the upper OMZ. This figure is comparable to the reduction in resting metabolic rate measured in the laboratory under these conditions.

Behavior of marine-mammal predators also suggests that *D. gigas* may be slowed down under OMZ conditions. Sperm whales in the Guaymas Basin in fall preferentially hunt near the upper OMZ during both day and night, possibly because escape responses and fast jetting of the squid are impaired, and the increase in probability of capture might outweigh the decreased probability of encounter (Davis et al., 2007). Data in the present study confirm that squid in the upper OMZ move much less rapidly than at more oxygenated depths, consistent with the mechanism proposed for this pattern of selective foraging. It remains unclear, though, to what extent escape responses are impaired under OMZ conditions. Escape-response behavior has not been studied in *D. gigas*, but the species possesses a specialized giant-axon system (Villegas, 1969) similar to that in loliginid squids where activation of giant axons is associated extremely powerful jets that are seldom, if ever, employed in conjunction with 'normal' locomotion like that studied here (Otis and Gilly, 1990).

Foraging under OMZ conditions?

Data in the present study show that *D. gigas* spends a great deal of time at midwater depths that are generally considered hypoxic ($<60\,\mu mol\,kg^{-1}$ oxygen), and in certain places and times occupancy extends to the upper boundary of the OMZ itself where oxygen concentrations are $<20\,\mu mol\,kg^{-1}$. Below this value, metabolic suppression reduces resting metabolism in *D. gigas* by ~80% at low temperatures (Gilly et al., 2006; Rosa and Seibel, 2008), and vertical velocities during rapid movements and depth-maintenance behavior *in vivo* are comparably reduced (Fig. 10). These results need to be evaluated in light of the fact that *D. gigas* must often be in the presence of a high concentration of micronektonic prey during the daytime at hypoxic depths.

Depth maintenance probably underlies much foraging behavior, and because of the relatively low vertical velocities involved, such activity might be metabolically feasible even in the upper boundary of the OMZ where metabolism is suppressed. The observed reduction of intermediate vertical velocities associated with depth maintenance in the upper OMZ – but not in the frequency of the behavior – is consistent with this idea. Depth maintenance thus appears to be an important activity that continues to be displayed under OMZ conditions but at greatly reduced vertical velocities. Such a strategy may be viable, because prey items encountered in this region are also likely to be lethargic. The lack of horizontal velocity information for *D. gigas* in nature represents a major limitation in our current knowledge.

It seems unlikely that the observed reductions in vertical velocity are severe enough to preclude consumption of lethargic prey in and just above the upper OMZ. ROV observations show that squid are capable of feeding under OMZ conditions (Zeidberg and Robison, 2007) (L.D.Z., unpublished data), but it remains unclear how often they do so, or whether they do so in the absence of artificial light. Low-light camera observations, particularly with an AVP approach, would provide an excellent way of documenting foraging at depth in areas of the Guaymas Basin (or further south in the Gulf) where the upper OMZ is close to (or even less than) the lower limit of the photic zone.

Daytime foraging at DSL/OMZ depths as suggested for *D. gigas* is hardly unique to this species. Many other top predators show repetitive diving behavior to depths occupied by the DSL during daytime (Dewar et al., 2011), including sperm whales (Davis et al., 2007), tunas (Schaefer and Fuller, 2010; Schaefer et al., 2011) and swordfish (Carey and Robison, 1981; Sepulveda et al., 2010; Dewar et al., 2011), all species that prey on or compete with *D. gigas*. Although utilization of this rich daytime foraging ground may be a common feature of many top pelagic predators, only *D. gigas* appears to be able to tolerate the relevant cold, hypoxic conditions

for several hours or more. Thus, the DSL/OMZ environment would appear to greatly favor *D. gigas*, and it is clearly an environment that this species inhabits and utilizes.

LIST OF ABBREVIATIONS

AVP	animal-borne video package
DML	dorsal mantle length
DSL	deep scattering layer
OLZ	oxygen limited zone
OMZ	oxygen minimum zone
PAT	pop-up archival transmitting
ROV	remotely operated vehicle

ACKNOWLEDGEMENTS

We thank Barbara Block and John O'Sullivan (Monterey Bay Aquarium) for continued support and access to Argos and data-archiving servers, Laurent Giovangrandi for MATLAB programs, Jorge Ramos-Castillejos for CTD casts in Santa Rosalia, Patrick Daniel for help with analyzing velocity distributions, and Sal Jorgenson, Gareth Lawson, Kelly Benoit-Bird and Brad Seibel for valuable discussions. We also acknowledge the invaluable assistance of captains and crews of all research vessels used: RV *New Horizon* (Scripps Institute of Oceanography), RV *BIPXII* (CIBNOR, Guaymas, Mexico), RV *Pacific Storm* (Bruce Mate, Oregon State University Marine Mammal Institute), the *Marylee* (John Barnes, La Paz, Mexico) and the *Sand Man* (Ron Steele, La Paz). We are grateful to Unai Markaida and Cesar Salinas for all manners of assistance in Mexico.

FUNDING

This work was supported by the National Science Foundation [grant numbers OCE 0526640, OCE60 0850839]; the David and Lucile Packard Foundation [grant numbers 2005-2800, 2008-32708]; the National Geographic Society [grant numbers 7578-04, 8458-08]; the Gordon and Betty Moore Foundation through the Census of Marine Life project, Tagging of Pacific Pelagics (TOPP); and National Geographic Television (Dangerous Encounters with Brady Barr).

REFERENCES

Alvarez-Borrego, S. and Lara-Lara, J. R. (1991). The physical environment and primary productivity of the Gulf of California. *Am. Assoc. Pet. Geol Memoir* **47**, 555-567.

Anderson, E. J. and DeMont, E. M. (2005). The locomotory function of the fins in the squid *Loligo pealei*. *Mar. Freshw. Behav. Physiol.* **38**, 169-189.

Argüelles, J., Rodhouse, P. G., Villegas, P. and Castillo, G. (2001). Age, growth and population structure of the jumbo flying squid *Dosidicus gigas* in Peruvian waters. *Fish. Res.* **54**, 51-61.

Azam, F. (1998). Microbial control of the oceanic carbon flux: the plot thickens. *Science* **280**, 694-696.

Bartol, I. K., Mann, R. and Patterson, M. R. (2001a). Aerobic respiratory costs of swimming in the negatively buoyant brief squid *Lolliguncula brevis*. *J. Exp. Biol.* **204**, 3639-3653.

Bartol, I. K., Patterson, M. R. and Mann, R. (2001b). Swimming mechanics and behavior of the shallow-water brief squid *Lolliguncula brevis*. *J. Exp. Biol.* **204**, 3655-3682.

Bartol, I. K., Krueger, P. S., Thompson, J. T. and Stewart, W. J. (2008). Swimming dynamics and propulsive efficiency of squids throughout ontogeny. *Integr. Comp. Biol.* **48**, 720-733.

Bazzino, G., Gilly, W. F., Markaida, U., Salinas-Zavala, C. A. and Ramos-Castillejos, J. (2010). Horizontal movements, vertical-habitat utilization and diet of the jumbo squid (*Dosidicus gigas*) in the Pacific Ocean off Baja California Sur, Mexico. *Progr. Oceanogr.* **86**, 59-71.

Benoit-Bird, K. J. and Gilly, W. F. (2012). Coordinated nocturnal behavior of foraging jumbo squid, *Dosidicus gigas*. *Mar. Ecol. Prog. Ser.* **455**, 211-228.

Benoit-Bird, K. J., Au, W. W. L. and Wisdom, D. W. (2009). Nocturnal light and lunar cycle effects on diel migration of micronekton. *Limnol. Oceanogr.* **54**, 1789-1800.

Boden, B. P. and Campa, E. M. (1967). The influence of natural light on the vertical migrations of an animal community in the sea. *Symp. Zool. Soc. Lond.* **19**, 15-26.

Carey, F. G. and Robison, B. H. (1981). Daily patterns in the activities of swordfish, *Xiphias gladius*, observed by acoustic telemetry. *Fish Bull.* **79**, 277-292.

Childress, J. J. and Seibel, B. A. (1998). Life at stable low oxygen levels: adaptations of animals to oceanic oxygen minimum layers. *J. Exp. Biol.* **201**, 1223-1232.

Davis, R. W., Jaquet, N., Gendron, D., Markaida, U., Bazzino, G. and Gilly, W. (2007). Diving behavior of sperm whales in relation to behavior of a major prey species, the jumbo squid, in the Gulf of California, Mexico. *Mar. Ecol. Prog. Ser.* **333**, 291-302.

Dawe, E. G., Beck, P. C., Drew, H. J. and Winters, G. H. (1981). Long distance migration of a short finned squid, *Illex illecebrosus*. *J. Northwest Atl. Fish. Sci.* **2**, 75-76.

Dewar, H., Prince, E. D., Musyl, M. K., Brill, R. W., Sepulveda, C., Luo, J., Foley, D., Orbesen, E. S., Domeier, M. L., Nasby-Lucas, N. et al. (2011). Movements and behaviors of swordfish in the Atlantic and Pacific Oceans examined using pop-up satellite archival tags. *Fish. Oceanogr.* **20**, 219-241.

Diaz, R. J. and Rosenberg, R. (1995). Marine benthic hypoxia: a review of its ecological effects and the behavioural responses of benthic macrofauna. *Oceanogr. Mar. Biol. Annu. Rev.* **33**, 245-303.

Drazen, J. C. and Seibel, B. A. (2007). Depth-related trends in metabolism of benthic and benthopelagic deep-sea fishes. *Limnol. Oceanogr.* **52**, 2306-2316.

Fiedler, P. C. and Talley, L. D. (2006). Hydrography of the eastern tropical Pacific: a review. *Prog. Oceanogr.* **69**, 143-180.

Field, J. C., Baltz, K., Phillips, A. J. and Walker, W. A. (2007). Range expansion and trophic interactions of the jumbo squid, *Dosidicus gigas*, in the California Current. *CCOFI Rep.* **48**, 131-146.

Forward, R. (1988). Diel vertical migration: zooplankton photobiology and behavior. *Oceanogr. Mar. Biol.* **26**, 361-392.

Gilly, W. F., Preuss, T. and McFarlane, M. B. (1996). All-or-none contraction and sodium channels in a subset of circular muscle fibers of squid mantle. *Biol. Bull.* **191**, 337-340.

Gilly, W. F., Markaida, U., Baxter, C. H., Block, B. A., Boustany, A., Zeidberg, L., Reisenbichler, K., Robison, B., Bazzino, G. and Salinas, C. (2006). Vertical and horizontal migrations by the jumbo squid *Dosidicus gigas* revealed by electronic tagging. *Mar. Ecol. Prog. Ser.* **324**, 1-17.

Helly, J. J. and Levin, L. (2004). Global distribution of naturally occurring marine hypoxia on continental margins. *Deep Sea Res. Part I* **51**, 1159-1168.

Hoar, J. A., Sim, E., Webber, D. M. and O'Dor, R. K. 1994. The role of fins in the competition between squid and fish. In *Mechanics and Physiology of Animal Swimming* (ed. L. Maddock, Q. Bone and J. M. V. Rayner), pp. 27-43. Cambridge: Cambridge University Press.

Hofmann, A. F., Peltzer, E. T., Walz, P. M. and Brewer, P. G. (2011). Hypoxia by degrees: establishing definitions for a changing ocean. *Deep Sea Res. Part I* **58**, 1212-1226.

Karstensen, J., Stramma, L. and Visbeck, M. (2008). Oxygen minimum zones in the eastern tropical Atlantic and Pacific oceans. *Prog. Oceanogr.* **77**, 331-350.

Levin, L. A. (2003). Oxygen minimum zone benthos: adaptations and community response to hypoxia. *Oceanogr. Mar. Biol. Annu. Rev.* **41**, 1-45.

Markaida, U. and Sosa-Nishizaki, O. (2003). Food and feeding habits of jumbo squid *Dosidicus gigas* (Cephalopoda: Ommastrephidae) from the Gulf of California, Mexico. *J. Mar. Biol. Assoc. UK* **83**, 507-522.

Markaida, U., Quiñónez-Velázquez, C. and Sosa-Nishizaki, O. (2004). Age, growth and maturation of jumbo squid *Dosidicus gigas* (Cephalopoda: Ommastrephidae) from the Gulf of California, Mexico. *Fish. Res.* **66**, 31-47.

Markaida, U., Gilly, W., Salinas-Zavala, C. A., Rosas-Luis, R. and Booth, J. T. A. (2008). Food and feeding of jumbo squid *Dosidicus gigas* in the Central Gulf of California during 2005-2007. *CalCOFI Rep.* **49**, 90-103.

Marshall, G., Bakhtiari, M., Shepard, M., Tweedy, J., III, Rasch, D., Abernathy, K., Joliff, B., Carrier, J. C. and Heithaus. (2007). An advanced solid-state animal-borne video and environmental data-logging ("Crittercam") for marine research. *Mar. Technol. Soc. J.* **41**, 31-38.

Nakamura, Y. (1993). Vertical and horizontal movements of mature females of *Ommastrephes bartramii* observed by ultrasonic telemetry. In *Recent Advances in Fisheries Biology* (ed. T. Okutani, R. K. O'Dor and T. Kubodera), pp. 331-336. Tokyo: Tokai University Press.

Nigmatullin, C. M., Nesis, K. N. and Arkhipkin, A. I. (2001). A review on the biology of the jumbo squid *Dosidicus gigas*. *Fish. Res.* **54**, 9-19.

O'Dor, R. K. (1982). Respiratory metabolism and swimming performance of the squid, *Loligo opalescens*. *Can. J. Fish. Aquat. Sci.* **39**, 580-587.

O'Dor, R. K. (1988). The forces acting on swimming squid. *J. Exp. Biol.* **137**, 421-442.

O'Dor, R. K. (2002). Telemetered cephalopod energetics: swimming, soaring, and blimping. *Integr. Comp. Biol.* **42**, 1065-1070.

O'Dor, R. K. and Webber, D. M. (1986). The constraints on cephalopods: why squid aren't fish. *Can. J. Zool.* **64**, 1591-1605.

O'Dor, R. K., Hoar, J. A., Webber, D. M., Carey, F. G., Tanaka, S., Martins, H. R. and Porteiro, F. M. (1994). Squid (*Loligo forbesi*) performance and metabolic rates in nature. *Mar. Freshw. Behav. Physiol.* **25**, 163-177.

Otis, T. S. and Gilly, W. F. (1990). Jet-propelled escape in the squid *Loligo opalescens*: concerted control by giant and non-giant motor axon pathways. *Proc. Natl. Acad. Sci. USA* **87**, 2911-2915.

Packard, A. (1969). Jet propulsion and the giant fibre response of *Loligo*. *Nature* **221**, 875-877.

Paulmier, A. and Ruiz-Pino, D. (2009). Oxygen minimum zones (OMZs) in the modern ocean. *Prog. Oceanogr.* **80**, 113-128.

Pennington, J. T., Mahoney, K. L., Kuwahara, V. S., Kolber, D. D., Calienes, R. and Chavez, F. P. (2006). Primary production in the eastern tropical Pacific: a review. *Prog. Oceanogr.* **69**, 285-317.

Ringelberg, J. (1995). Changes in light intensity and diel vertical migration: a comparison of marine and freshwater environments. *J. Mar. Biol. Assoc. UK* **75**, 15-25.

Roper, C. F. E., Sweeney, M. J. and Nauen, C. E. (1984). FAO species catalogue. Cephalopods of the World. An annotated and illustrated catalogue of species of interest to fisheries. Vol. 3. FAO Fisheries Synopsis. Rome: FAO.

Rosa, R. and Seibel, B. A. (2008). Synergistic effects of climate-related variables suggest future physiological impairment in a top oceanic predator. *Proc. Natl. Acad. Sci. USA* **105**, 20776-20780.

Rosa, R. and Seibel, B. A. (2010). Metabolic physiology of the Humboldt squid, *Dosidicus gigas*: implications for vertical migration in a pronounced oxygen minimum zone. *Prog. Oceanogr.* **86**, 72-80.

Schaefer, K. M. and Fuller, D. W. (2010). Vertical movements, behavior, and habitat of bigeye tuna (*Thunnus obesus*) in the equatorial eastern Pacific Ocean, ascertained from archival tag data. *Mar. Biol.* **157**, 2625-2642.

Schaefer, K. M., Fuller, D. W. and Block, B. A. (2007). Movements, behavior, and habitat utilization of yellowfin tuna (*Thunnus albacares*) in the northeastern Pacific Ocean, ascertained through archival tag data. *Mar. Biol.* **152**, 503-525.

Schaefer, K. M., Fuller, D. W. and Block, B. A. (2011). Movements, behavior, and habitat utilization of yellowfin tuna (*Thunnus albacares*) in the Pacific Ocean off Baja California, Mexico, determined from archival tag data analyses, including unscented Kalman filtering. *Fish. Res.* **112**, 22-37.

Sepulveda, C. A., Knight, A., Nasby-Lucas, N. and Domeier, M. L. (2010). Fine-scale movements of swordfish *Xiphias gladius* in the Southern California Bight. *Fish. Oceanogr.* **19**, 279-289.

Stark, K. E., Jackson, G. D. and Lyle, J. M. (2005). Tracking arrow squid movements with an automated acoustic telemetry system. *Mar. Ecol. Prog. Ser.* **299**, 167-177.

Villegas, G. M. (1969). Electron microscopic study of the giant nerve fiber of the giant squid *Dosidicus gigas*. *J. Ultrastruct. Res.* **26**, 501-514.

Webber, D. M., Aitken, J. P. and O'Dor, R. K. (2000). Costs of locomotion and vertic dynamics of cephalopods and fish. *Physiol. Biochem. Zool.* **73**, 651-662.

Weihs, D. (1973). Mechanically efficient swimming techniques for fish with negative buoyancy. *J. Mar. Res.* **31**, 194-208.

Yano, K., Ochi, Y., Shimizu, H. and Kosuge, T. (2000). Diurnal swimming patterns of the diamondback squid as observed by ultrasonic telemetry. In *Biotelemetry 15: Proceedings of the 15th International Symposium on Biotelemetry, Juneau, Alaska, USA, May 9-14, 1999* (ed. J. H. Eiler, D. J. Alcorn and M. R. Neuman), pp. 108-116. Wageningen: International Society on Biotelemetry.

Yatsu, A., Yamanaka, K. and Yamashiro, C. (1999). Tracking experiments of the jumbo flying squid, *Dosidicus gigas*, with an ultrasonic telemetry system in the Eastern Pacific Ocean. *Bull. Nat. Res. Inst. Far Seas Fish.* **36**, 55-60.

Zeidberg, L. D. and Robison, B. H. (2007). Invasive range expansion by the Humboldt squid, *Dosidicus gigas*, in the eastern North Pacific. *Proc. Natl. Acad. Sci. USA* **104**, 12948-12950.